5th INTERNATIONAL MAAR CONFERENCE

Monogenetic volcanism of the Michoacán-Guanajuato Volcanic Field: Maar craters of the Zacapu basin and domes, shields, and scoria cones of the Tarascan highlands (Paracho-Paricutin region)

Pre-meeting field guide for the
5th International Maar Conference, Querétaro, México

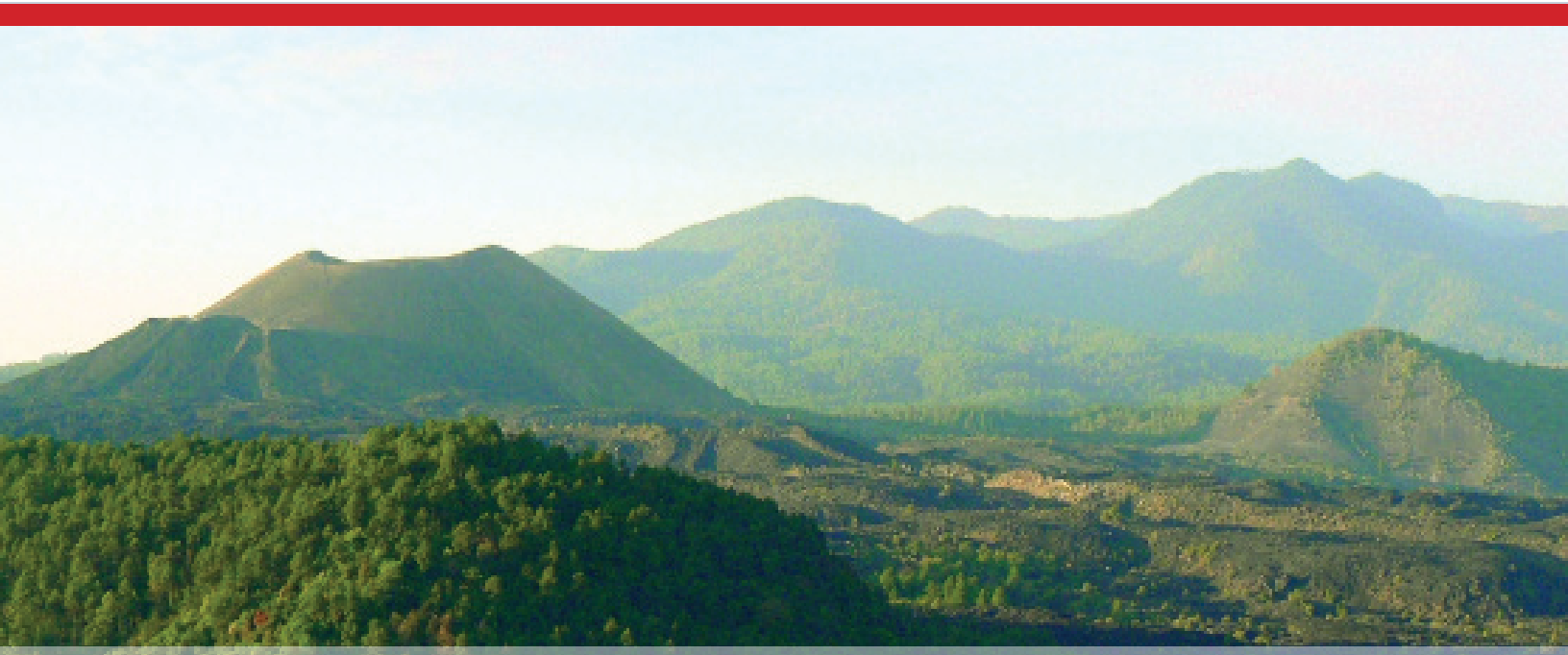

Claus Siebe, Marie-Noelle Guilbaud, Sergio Salinas, Pooja Kshirsagar,
Magdalena Oryaelle Chevrel, Juan Ramón de la Fuente,
Athziri Hernández Jiménez, and Lourdes Godínez

Departamento de Vulcanología, Instituto de Geofísica, Universidad Nacional Autónoma de México

November 13-17, 2014

Cover description: Panoramic view of the Paricutin Volcano (left) from the terrace of Angahuan tourist center, See the text and Figure 37 of this guide for more details.

Monogenetic volcanism of the Michoacán-Guanajuato Volcanic Field: Maar craters of the Zacapu basin and domes, shields, and scoria cones of the Tarascan highlands (Paracho-Paricutin region)

A pre-meeting fieldtrip (November 13-17) prior to the 5th International Maar Conference (5IMC-IAVCEI), Querétaro, Mexico, November 17-22, 2014

Leaders: Claus Siebe, Marie-Noëlle Guilbaud, Sergio Salinas, Pooja Kshirsagar, Magdalena Oryaëlle Chevrel, Juan Ramón de la Fuente, Athziri Hernández Jiménez, and Lourdes Godínez

Departamento de Vulcanología, Instituto de Geofísica, Universidad Nacional Autónoma de México

csiebe@geofisica.unam.mx, m.guilbaud@geofisica.unam.mx, sss@geofisica.unam.mx, pooja6vulcan@gmail.com, oryaelle.chevrel@gmail.com, jrdfr86@gmail.com, axiriss@gmail.com, lgodinez@unam.mx

ABSTRACT

The Michoacán-Guanajuato Volcanic Field in the Trans-Mexican Volcanic Belt contains the largest concentration of monogenetic vents on Earth associated with a subduction-related continental arc, holding more than 1,100 edifices consisting of abundant scoria cones, about 300 "enigmatic" shields, and ~22 maars. Paricutin (1943-1952) is the youngest volcano of this field and together with Jorullo (1759-1774) the only monogenetic volcano formed since the Spanish conquest (1519-1521) in the Trans-Mexican Volcanic Belt. Both volcanoes are said to be monogenetic because they were produced entirely by single eruptions and hence will presumably never erupt again. Nonetheless, another monogenetic eruption will certainly occur again and form a new scoria cone on Mexican ground. In order to minimize losses of life and property it is desirable to learn more about these types of eruptions and with this knowledge design preventive strategies. In recent years it has become clear that monogenetic eruptions can be quite diverse in style and duration. For this reason, we will visit different examples of monogenetic volcanoes (maars, scoria cones, shields, domes) to cover the entire spectrum of monogenetic volcanism and discuss the possible causes of its eruptive variability. This guidebook is designed as a companion for a pre-meeting field trip but might also be a handy tool for those wishing to visit the area with condensed and updated information at hand. The guide contains excursions to the maars of the Zacapu basin (1 day/ 1 night), scoria cones, domes, and shields in the Cherán-Paracho region (1 day/ 1 night) and historic Paricutin volcano and immediate surroundings (2 days/ 2 nights), with overnight stays at Zacapu and Uruapan. The trip starts at Morelia and ends at Querétaro.

INTRODUCTION: SCORIA CONES, MAARS, AND MEDIUM-SIZED VOLCANOES (SHIELDS AND DOMES) IN THE MICHOACÁN-GUANAJUATO VOLCANIC FIELD

This fieldtrip guide is devoted to Particutin and other monogenetic volcanoes in western-central Mexico, an area that can be easily reached on paved roads from Morelia, the capital city of Michoacán (Figs. 1, 2). It partly follows up and is complementary to a previous guide (Guilbaud et al., 2009) that was in great part devoted to the historic eruption (1759-1774) of Jorullo volcano, located to the south.

The subduction-related Trans-Mexican Volcanic Belt (TMVB) is ~1200 km long and traverses central Mexico in an E-W direction from the Gulf of Mexico to the Pacific coast. The TMVB includes several dozen strato-volcanoes, calderas, domes, as well as >3000 monogenetic edifices. The highest concentration of monogenetic volcanoes occurs in its western-central part, where the arc reaches a maximum width of 150 km (Fig. 3). This ~40,000 km^2 area, the Michoacán-Guanajuato Volcanic Field (MGVF), hosts more than 1100 monogenetic vents, and the only two volcanoes born in historical times in the TMVB: Jorullo (1759-1774) and Paricutin (1943-1952). In addition to the >1100 monogenetic scoria cones and associated lava flows, ~300 shield volcanoes, tens of lava domes, and 22 phreato-magmatic vents (maars and tuff cones) have been identified (Hasenaka and Carmichael, 1985 and Hasenaka et al., 1994). Large strato-volcanoes that are so typical for subduction-related arcs are mostly absent in the MGVF. The only true strato-volcanoes recognized so far in this region are Tancítaro (3845 m) and Patamban (3450 m). Tancítaro is believed to be extinct (Ownby et al., 2006), while Patamban has never been studied in detail.

TMVB volcanism has existed in the MGVF since at least 5 Ma producing predominantly calc-alkaline andesites, displaying a wide range in compositions (olivine basalts to rhyolites, including exotic alkaline varieties, e.g. Hasenaka et al., 1987). The fame of the MGVF is mostly related to the fact that it hosts Paricutin, a scoria cone born in a corn-field in 1943. This eruption lasted until 1952 and motivated the first modern volcanological studies in the area (Luhr and Simkin, 1993, and references therein). Most of these works focused on Paricutin, and few addressed the regional volcanic geology of the area (Williams, 1950). First comprehensive studies considering the entire MGVF include those by Hasenaka and Carmichael (1985; 1987), followed by Connor (1987),

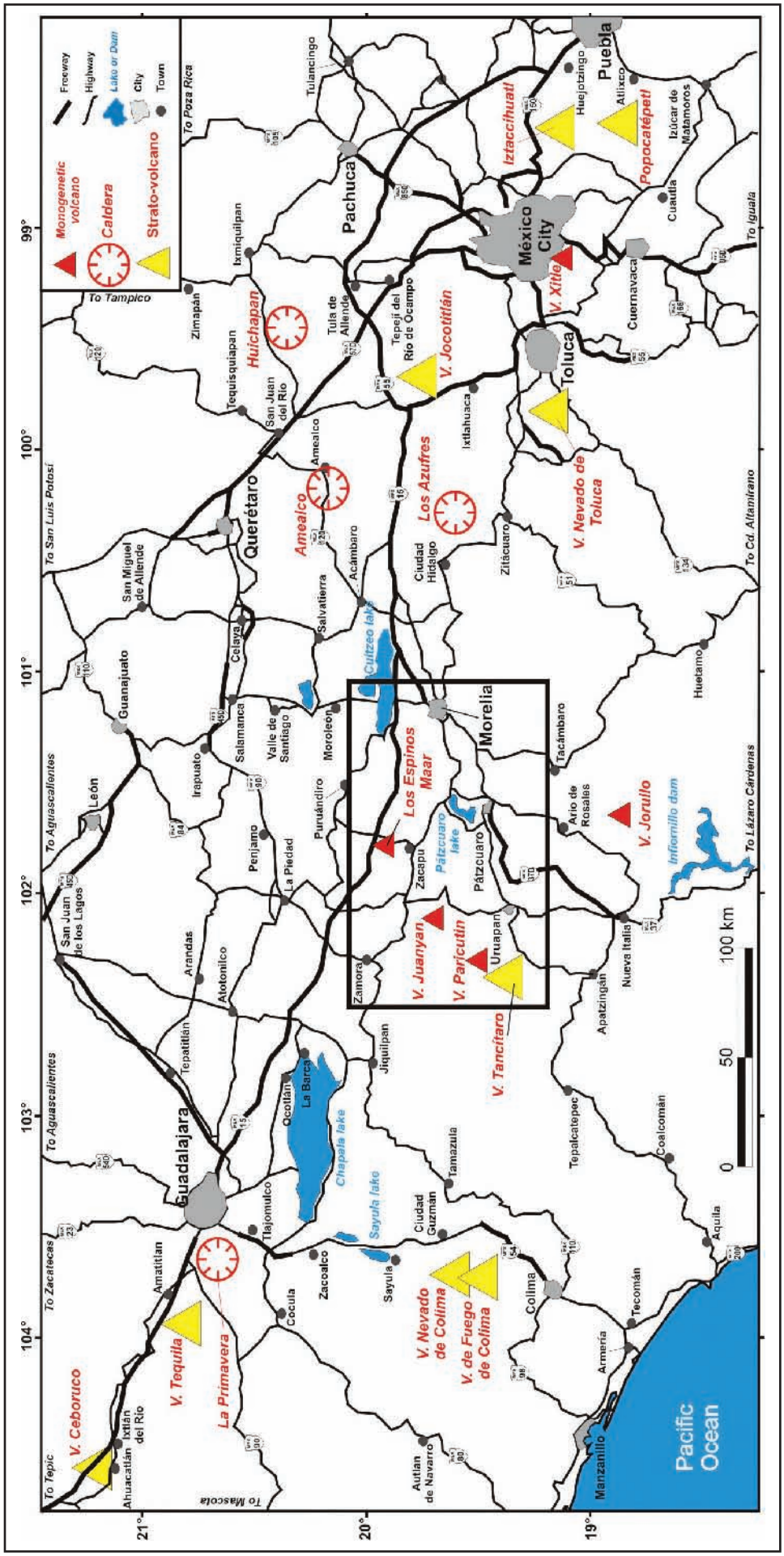

Figure 1: Road map showing fieldtrip area (outlined by rectangle) and its location within central México. Major volcanoes are indicated.

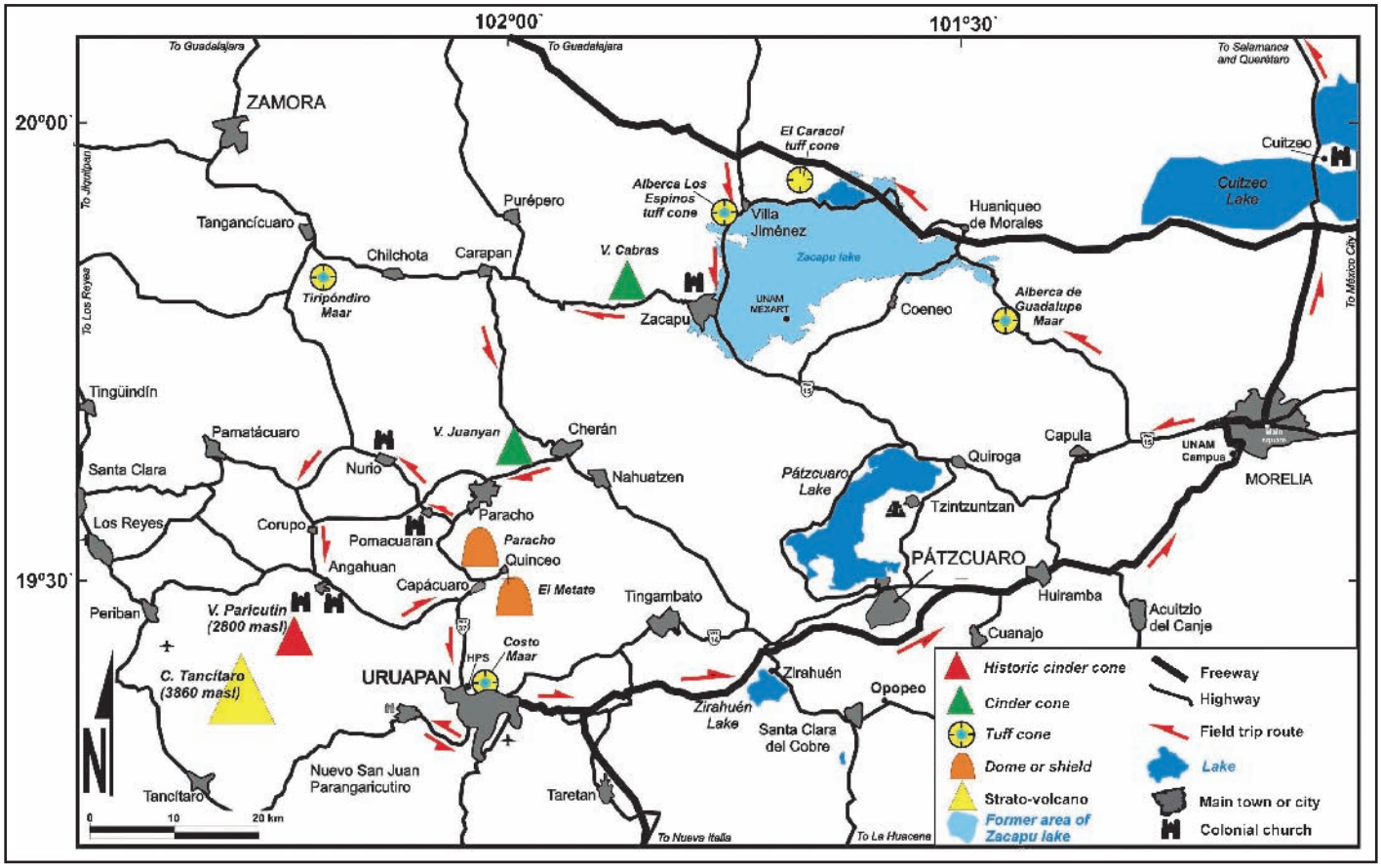

Figure 2: Road map of the itinerary showing main cities and towns (Morelia, Zacapu, Cherán, Paracho, Angahuan, Uruapan, Pátzcuaro, Cuitzeo, Querétaro) and volcanoes to be visited.

Ban et al. (1992), Roggensack (1992), Hasenaka (1994), and Hasenaka et al. (1994). Some conclusions reached by these authors (e.g. the southward migration of volcanic activity) remain debatable due to the lack of sufficient reliable information (especially radiometric dates and estimated eruption volumes). Because of the large extent of the MGVF and remoteness of some sectors, detailed mapping and radiometric dating were not undertaken until recently. First detailed maps and systematic radiometric age data sets of discrete areas were published by Ownby et al. (2006, 2011) for the Tancítaro-Nueva Italia area and by Guilbaud et al. (2011, 2012) and Maciel-Peña et al. (2014) for the Jorullo and Tacámbaro-Puruarán areas. However, these areas are located near the volcanic front and the present fieldtrip focuses on the Zacapu basin and Paracho-Cherán (Tarascan highland) areas, located in the heartland of the MGVF. Following the same methodology as employed in the recent works, we are now analyzing the composition and mineralogy (petrography, major and trace elements, Sr-Nd-Pb isotopes) and determining radiometric ages (^{14}C, $^{40}Ar/^{39}Ar$) at as many volcanoes within this area as possible. With this new data in hand, we will determine with greater precision eruption rates and compositional trends over time. Comparison with previous results from areas located towards the arc front will allow us to test hypotheses about the origin and evolution of the entire MVGF (e.g. Siebe et al., 2013). Furthermore, we will be able to better estimate the probability of recurrence of volcanic activity in this area. So far, preliminary results of our studies indicate that volcanism has not migrated southward in this region, as often postulated, but rather has become more intense at the arc front (e.g. we have found that during the Holocene, at least 13 eruptions occurred in the Tacámbaro area which yields an average recurrence interval of 800 years, one of the highest monogenetic eruption frequencies detected within such a small area in a subduction-setting). Compositions of erupted products are distinctly more diverse and less evolved at the arc front (high proportion of basaltic andesites and occurrence of exotic alkaline compositions in the Tacámbaro area) than at greater distances from the trench (mostly andesites, but also dacites and rhyolites in the Zacapu basin and Tarascan highlands). Volcanic centers are preferentially aligned along SW-NE directions (N50°) in the Tacámbaro área compared to WSW-ENE (N80°) in the Zacapu basin, consistent with local fault strikes. A higher rate of lithospheric extension in the south during the Quaternary seems to have allowed a larger number of small, poorly evolved, and compositionally diverse dikes to reach the surface during this period.

As mentioned above, over 1100 volcanic centers in the MGVF are small monogenetic scoria cones (few rare maars occur also) formed by Strombolian eruptions and associated lava flows. Another 400 are described as medium-sized volcanoes with a much larger volume (between 0.5 and 10 km^3, and up to 50 km^3) than scoria cones (average of 0.021 km^3; Hasaneka and Carmichael, 1985; Hasenaka, 1994; Roggensack, 1992). These medium-sized volcanoes are an important part of the landscape and deserve more attention than they have received so far, especially because their nature is not clear. Most of them were recognized as shields (shaped predominantly by effusive activity) crowned by a small lava dome or scoria cone, and others as composite (e.g. cones

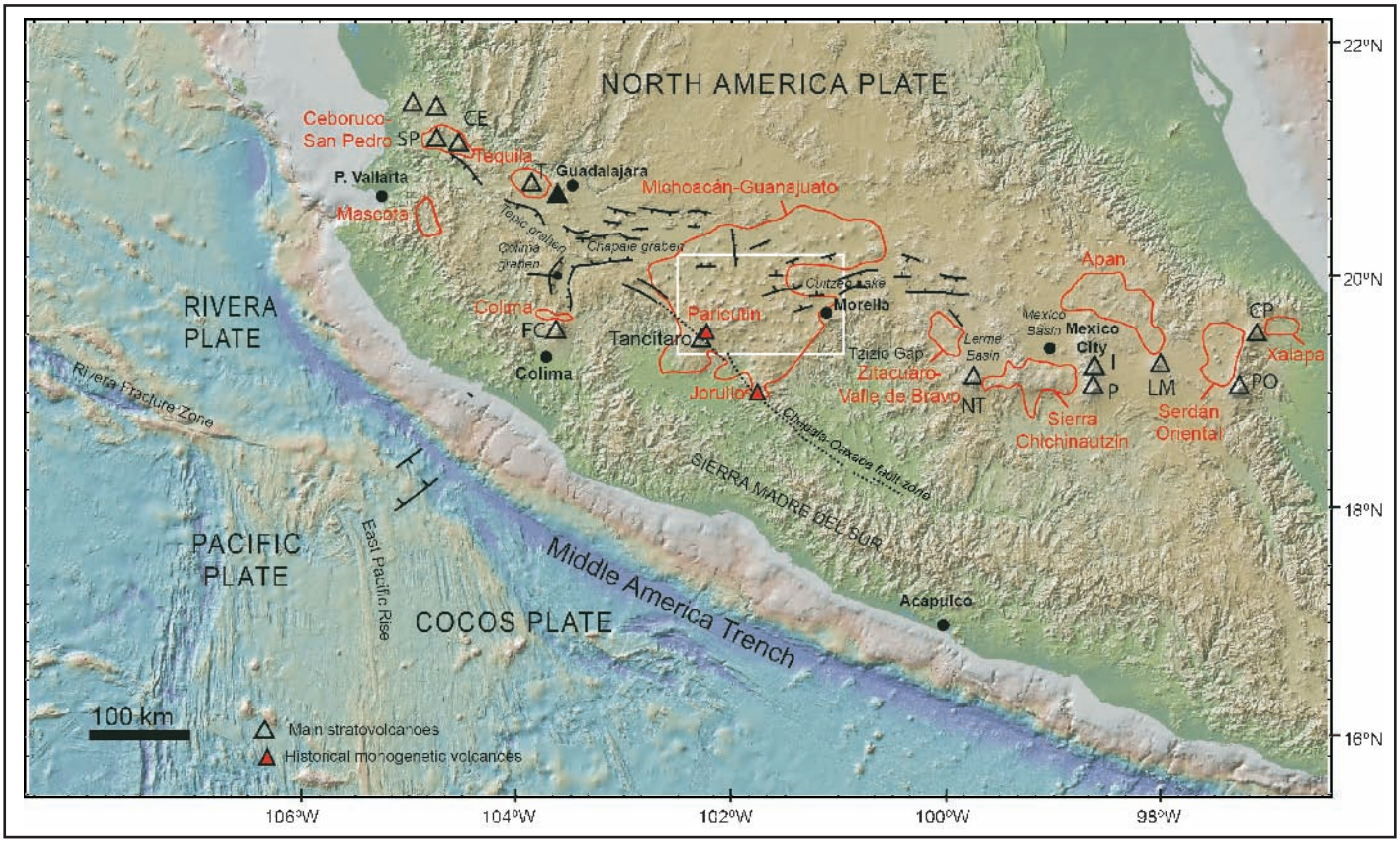

Figure 3: Map of central Mexico showing monogenetic fields (red outlines) of the Trans-Mexican Volcanic Belt. White rectangle denotes area within the Michoacán-Guanajuato Volcanic Field to be visited during the excursion. Major cities and main tectonic features are also indicated. Strato-volcanoes: SP=San Pedro, CE=Ceboruco, T=Tequila, FC=Fuego de Colima, NT=Nevado de Toluca, I=Iztaccíhuatl, P=Popocatépetl, LM=La Malinche, PO=Pico de Orizaba, CP=Cofre de Perote.

or domes built partly by lava flows and partly by pyroclastic deposits; Hasenaka, 1994). Their morphology is particularly interesting because their slope angles are on average <10°, a figure that is similar or slightly steeper than that for Icelandic shields (Hasenaka 1994). However, unlike typical shields made of multiple thin basaltic flows, many shields in the MGVF are made of thick A'a to blocky andesite flows. Besides volume, differences in the rheological parameters (e.g. density, viscosity, chemical composition of the magma and its volatile content, eruption temperature, amount of crystals, and the pressure gradient that is controlling bubble nucleation, etc.) must exist between magmas giving rise to medium-sized volcanoes (e.g. effusive shields, domes, and composite edifices) and scoria cones to explain their specific eruption styles and resulting differences in volcanic edifice morphology. Since the geochemical differences between both volcano types seem to be restricted in many cases to subtle variations, further investigations focusing on the physical parameters are needed to clear the question of their marked differences in eruption style.

Finally, in contrast to the pervasively abundant scoria cones, only about two dozen phreato-magmatic monogenetic constructs (tuff rings, tuff cones, maars) have been identified in the MGVF (Siebe and Salinas, 2014). One half of these form a cluster near Valle de Santiago in the Lerma river valley at the northern margin of the MGVF (e.g. Aranda-Gómez et al., 2013), while the others occur in a more scattered fashion. The scarcity of this type of volcano (only ~2% of all monogenetic volcanoes in the MGVF) is striking and implies that conditions favoring their formation are rarely met in this region.

From the preceding introductory paragraphs it becomes clear that many questions in regard to the origin and nature of volcanism in the MGVF remain open. Those outlined above are only a few of the many issues that will be discussed during this fieldtrip.

LATE PLEISTOCENE PHREATO-MAGMATIC MAARS AND TUFF CONES OF THE ZACAPU BASIN (1 DAY, 1 NIGHT)

The first day of the excursion will be devoted to phreato-magmatic craters occurring in the periphery of the Zacapu lacustrine basin. This large intermontane basin (1980 masl) has a total catchment area of ~1480 km^2 and owes its origin to a tectonic graben formed by an ENE-WSW trending domino-style extensional fault system (Fig. 4). The basin has been of interest for its archaeological (Pétrequin, 1994; Pereira, 2005), paleo-climatical (Metcalfe, 1992; 1995; Telford et al., 2004; Newton et al., 2005), and volcanological records (e.g. Demant, 1992; Siebe et al., 2012). Studies indicate that the lake was originally larger and deeper than today, but turned at times marshy during the Quaternary (Tricart, 1992; Ortega et al., 2002). It possessed a shallow discharge and water canals (Correa-Metrio et al., 2012) until the lake was artificially drained in the late 19th century to gain fertile land for agricultural purposes (Noriega and Noriega, 1923; Telford et al., 2004; Siebe et al., 2012). The small city of Zacapu (or Tzacapu, place of stones in Purhépecha language) is located at the SW margin of the basin ~80 km NW of Morelia. This region is

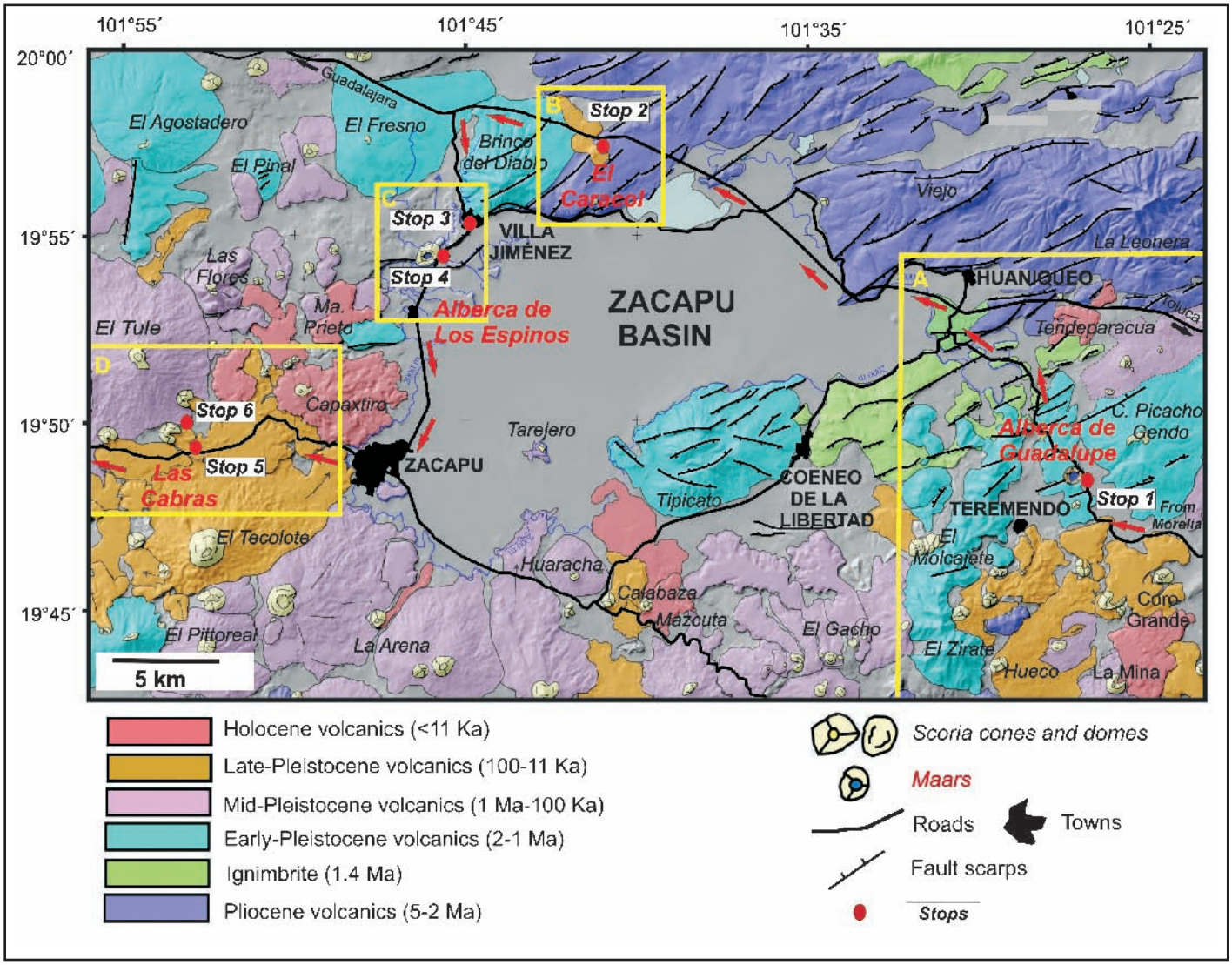

Figure 4: Simplified geologic map of the Zacapu intermontane lacustrine basin showing travel route (red arrows) and Stops 1 to 6 to be visited during the first part of the excursion. Yellow rectangles A, B, C, and D denote areas covered by detailed maps in Figs. 5, 9, 16, and 19, respectively.

characterized by two main landforms: the intermontane lakes and the surrounding volcanic highlands. The climate (average annual temperature = 17°C, precipitation ~850 mm/yr) is dominated by northwesterly winds that provide a mostly dry weather during the major part of the year.

After the Spanish conquest the aboriginal Purhépecha dwellers of the area were embraced by the Catholic faith in 1548 under the leadership of the Franciscan friar Fray Jacobo Daciano who initiated the building of a church in Zacapu that was entrusted to the patronage of the Apostle Peter. Agriculture currently encompasses 47% of the total basin persisting due to the presence of several natural springs with high discharge rate and a system of irrigation canals (observable at Villa Jiménez, Fig. 4). Pine and oak forests grow in the volcanic highlands that surround the basin, with the occasional occurrence of tropical deciduous forests on the eastern slopes and grasslands restricted to the southwestern part of the basin.

DAY 1: PHREATO-MAGMATIC VENTS OF THE ZACAPU BASIN: ALBERCA DE GUADALUPE, EL CARACOL, AND ALBERCA DE LOS ESPINOS

During this day three of the few phreatomagmatic monogenetic vents encountered in the entire MGVF will be visited. All three of them occur in the periphery of the Zacapu basin (Figs. 2, 4) to which they are genetically linked by the availability of sufficient ground-and/or-surface water required for their formation. During the morning, Alberca de Guadalupe maar (Stop 1) and El Caracol tuff cone (Stop 2) will be visited (Fig. 4). Then, we will drive to Villa Jiménez (Stop 3 at water canal) and Alberca de los Espinos tuff cone where we will have lunch at the crater rim (Stop 4A) before visiting several quarries at its outer slopes (Stops 4B-4C). The night will be spent in Zacapu.

Itinerary: Leave the main square of Morelia on Av. Francisco Madero in the direction of Capula and Quiroga to the west (Fig. 2). This avenue further transforms into federal highway No. 15. After passing several new social housing complexes, at ~15 km (25 Mins.) turn right (north) at the natural gas storage facility and continue on state highway towards Cuto de Esperanza and Huaniqueo. To the left several remnants of quarried scoria cones can be seen (see also photo on inner back cover). About 30 years

ago these cones were still intact before extensive quarrying for building materials led to their almost complete destruction. Today most of the quarries are being used as garbage dumps for the city of Morelia. Further on along this route, the heterogeneity in the young volcanic landforms can be viewed at several late Pleistocene-Holocene scoria cones like La Mina, Sajo Grande, Coro Grande, etc. Early Pleistocene El Zirate dome complex (3345 m) and Picacho Gendo shield (2550 m) are easily visible from the road. Continue on this route and after a drive of ~23 km (25 Mins.) arrive at the eastern crater rim (terrace with panoramic view at Guadalupe town) of the Alberca de Guadalupe maar crater (Stop 1). The view allows grasping fundamental issues related to the phenomenon of maar formation, as one can see that the crater literally forms a hole in the otherwise relatively planar topography of the early Pleistocene lava flows. To the left from the panoramic view point a small road leads down to the crater lake along which typical maar deposits can be observed (see description below).

From here, drive north towards Huaniqueo for ~14 km (19 Mins.) and arrive on the federal freeway and continue from toll station in the direction of Guadalajara. After ~20 km (15 Mins.) and after crossing the lacustrine flats of the NE Zacapu paleo-lake followed by a continuous ascent along the northern Zacapu graben shoulder, arrive at Stop 2. On the left side of the freeway large quarries exposing the phreato-magmatic deposits of El Caracol can be seen (Figs. 2, 4). Halt the automobile off the freeway on the right side and approach the opposite side on foot with caution. Jump across the barbwire fence to have a closer view of the deposits (see description of Stop 2).

After having a look at the deposits of El Caracol, continue on the freeway in the direction of Guadalajara for ~9 km (7 Mins.) and exit the toll station in the direction of Zacapu. Then, drive south towards Villa Jiménez for ~7 km (9 Mins.) and stop at the bridge over the canal (Stop 3; Fig. 4).

From here, continue driving west towards Zacapu for ~4 km (5 Mins.) and arrive at the outer southern slope of Alberca de los Espinos tuff cone (Stop 4). From the parking lot, climb on foot to the crater rim (Stop 4A, good place for lunch) and enjoy the panoramic view of the crater lake and surrounding volcanic landforms. The plains of the former Zacapu lake and the present outlet of the lacustrine basin (canal at Villa

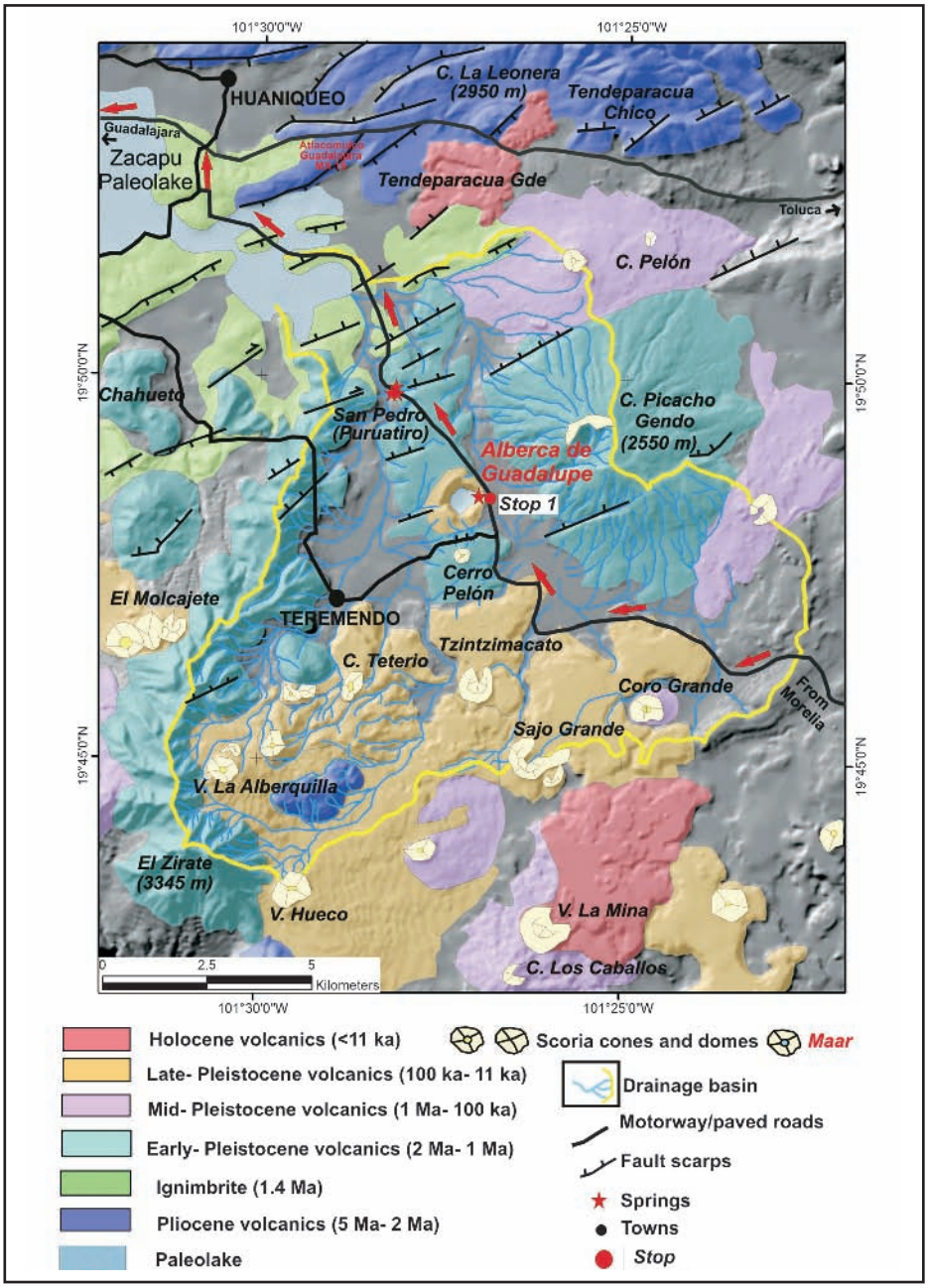

Figure 5: Geological map of the eastern Zacapu lake basin and location of Alberca de Guadalupe maar crater in the middle of a tributary drainage network. Red arrows denote travel route.

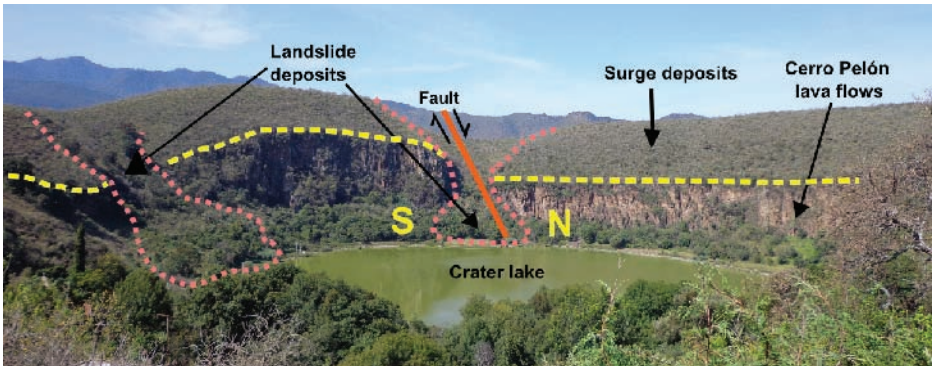

Figure 6: View of Alberca de Guadalupe maar from its eastern crater rim (Stop 1) towards the W. Phreatomagmatic deposits produced by the eruption cover an older lava flow (vertical cliff) from Cerro Pelón scoria cone. Normal fault and vertical displacement of ~ 20 m between southern (S) and downthrown northern (N) block are clearly visible. Post-eruption landslides contributed to further increase the width of the crater. Lake is ~9 m deep.

Jiménez) can also be observed. After lunch, two major quarries displaying the phreato-magmatic deposits (Stops 4B and 4C) will be visited. Later, drive for ~8 km (15 Mins.) to the hotel "Villa Zacapu", where we will stay for the night. If time allows, the 16th century church at the main square of Zacapu is worth visiting for its early colonial architecture.

Stop 1: Alberca de Guadalupe maar crater (19°48'28.70", 101°26'56.43", 2141 m)

The view-point displays a wide crater (~1 km in diameter) with a depth of ~140 m that bears a lake (~9 m deep), formed between 20,000 and 23,000 yr. BP ago. It is the youngest of the three phreato-magmatic constructs occurring within the Zacapu basin. It originated by perforating early Pleistocene lava flows from nearby Cerro Pelón. The northern block of the crater wall is down-thrown ~30 m by an E-W trending regional normal fault that has been active since Pliocene times (Figs. 5, 6, see also photo on front cover).

This unusual phreato-magmatic construct, in the semi-arid highlands of Zacapu, was favored by local hydrological and topographical conditions, especially the shallow aquifer parameters (e.g. high permeability and flow direction) that allowed funneling enough ground-and-surface water along narrow valleys to the eruption site in order to fuel continuous phreato-magmatic explosions. Today, shallow groundwater conditions still prevail as exemplified by several high-discharge springs near Puruátiro (~3 km NNW from the maar crater) and on the ENE inner wall of the crater, within the contact of the lava flows and the overlying surge deposits (Fig. 5), making it feasible that such an event could occur again.

The maar deposits are observable along the small paved road to the left of the viewing point that leads down to the crater lake. A well-stratified sequence of alternating dry and wet surge deposits that are disrupted by several ballistic lithics (angular andesite lava and ignimbrite clasts), displaying decimeter-scale impact sags (Figs. 7, 8), can be seen. The dry surge deposits are friable and consist of medium-to-coarse lapilli, that is mainly clast-supported, and poorly sorted (Mdφ: -1.56 to -3.75, σφ: 1.43 to 3.23). In contrast, the wet surge deposits are fairly indurated and consist of thin stratified layers of fine ash with accretionary lapilli (~1

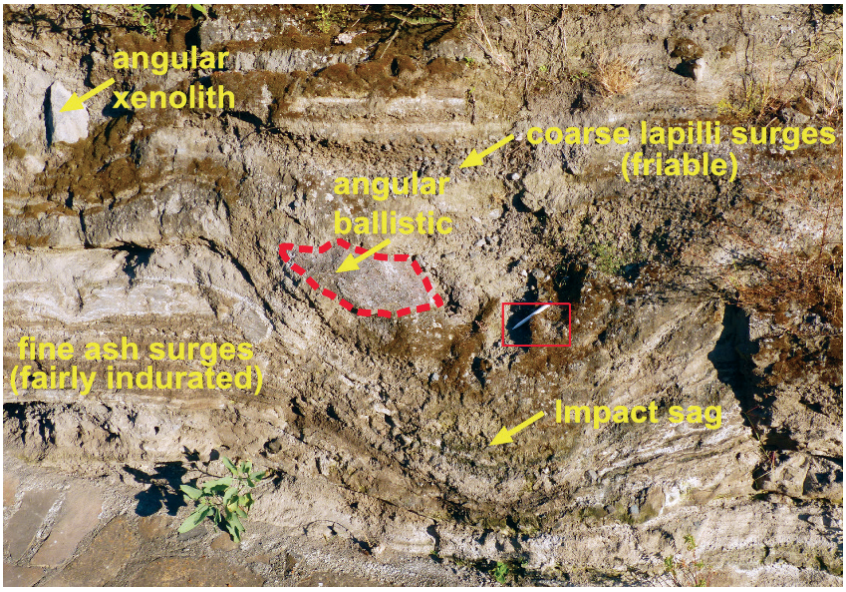

Figure 7: Typical surge deposits with ballistic impact sags observable at outcrop on the road leading from the crater rim down to the lake of Alberca de Guadalupe maar. Pen for scale (~18 cm) inside red rectangle.

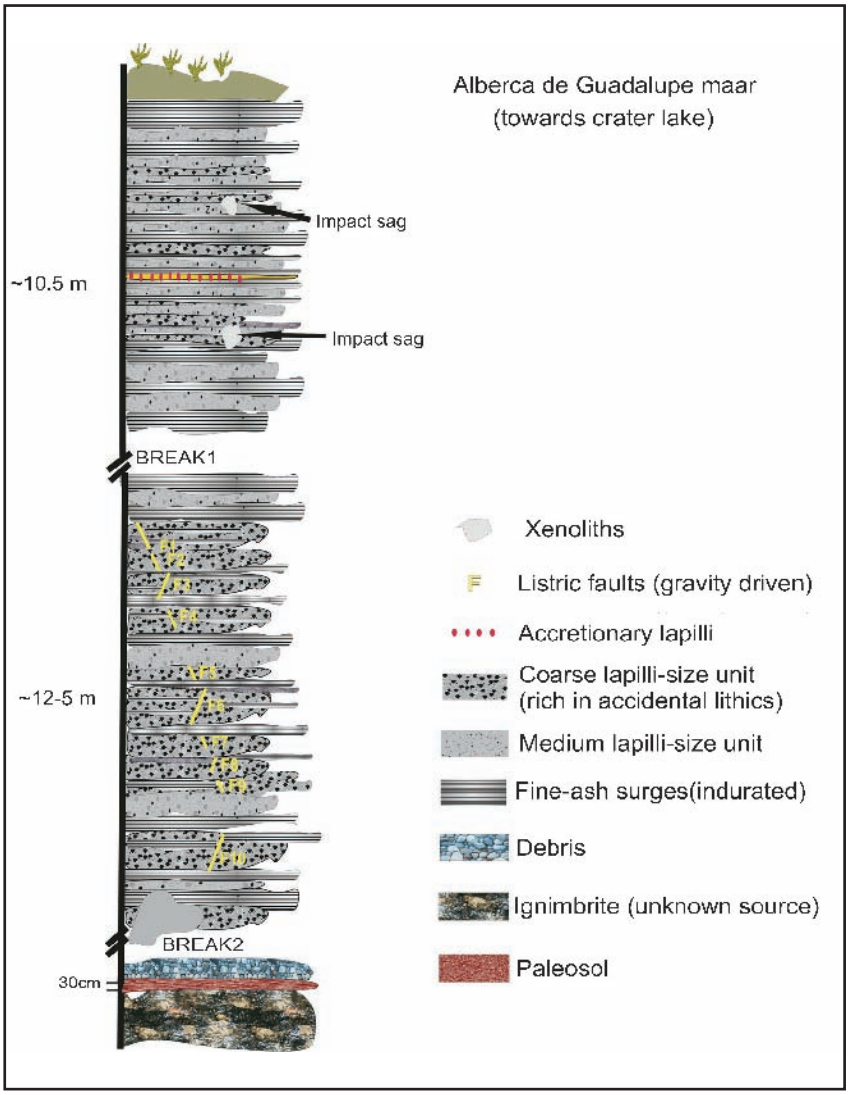

Figure 8: Stratigraphic sequence (mostly phreato-magmatic surge deposits) of Alberca de Guadalupe maar exposed at cuts encountered along road leading from the viewing point (Stop 1) at the eastern crater rim down to the lake.

cm in diameter). The deposits are poor in juveniles (cauliflower-type bombs of basaltic andesite, SiO_2=54-58 wt.%) that only constitute 12-49% of the deposits. Note the detailed characteristics of these deposits, since the deposits that will be encountered later during this day at the El Caracol and Alberca de los Espinos tuff cones bear some resemblances, but also some noteworthy differences (Kshirsagar et al., 2014).

Stop 2: El Caracol: A phreato-magmatic tuff cone associated with a scoria cone and lava flows (19°57'34.98", 101°40'52.70", 2055 m)

The unusual shape of this late Pleistocene landform consisting of a ~1 km-wide crater and associated lava flows inspired its name El Caracol (Spanish for snail). The eruption of this monogenetic vent ~28,000 yr. BP commenced with phreatomagmatic activity that formed a tuff cone and later transformed into dry-magmatic fountaining with formation of a small scoria cone at the NW rim of the tuff cone crater and the effusion of lava. The flows first filled the tuff-cone crater and subsequently poured over its NW rim, before covering the adjacent NW lower slopes and inundating nearby plains reaching a distance of 4.7 km from source (Figs. 9, 10). These basaltic andesite Aa-type flows (SiO_2=56 wt%) covered an area of ~4.7 km^2 with an estimated volume of 0.07 km^3. The eruptive sequence (Figs. 11, 12, 13) indicates that after a short phreatomagmatic prelude that built the tuff cone, the eruption soon turned magmatic. Although the vent is located not far from the Zacapu lake, the dry nature of the second phase of the eruption points toward insufficient availability of ground water to continue fueling phreatomagmatic activity. It seems that the permeability and groundwater flow gradient in the underlying aquifers (hard substrate of faulted Pliocene volcanics) are such that a continuous supply of water to the eruption site was not possible.

The crater is located on a small mesa (flat topographic high) well above tha Zacapu plains and sits along a normal NE-SW trending regional fault scarp (Fig. 10) that bounds a tectonically elevated horst of Pliocene lavas. This fault directed the ascending batch of magma that must have encountered water-saturated rocks shortly before reaching the surface.

The proximal deposits forming the tuff cone (Figs. 11, 12, 13) are predominantly phreatomagmatic fallout units rich in juve-

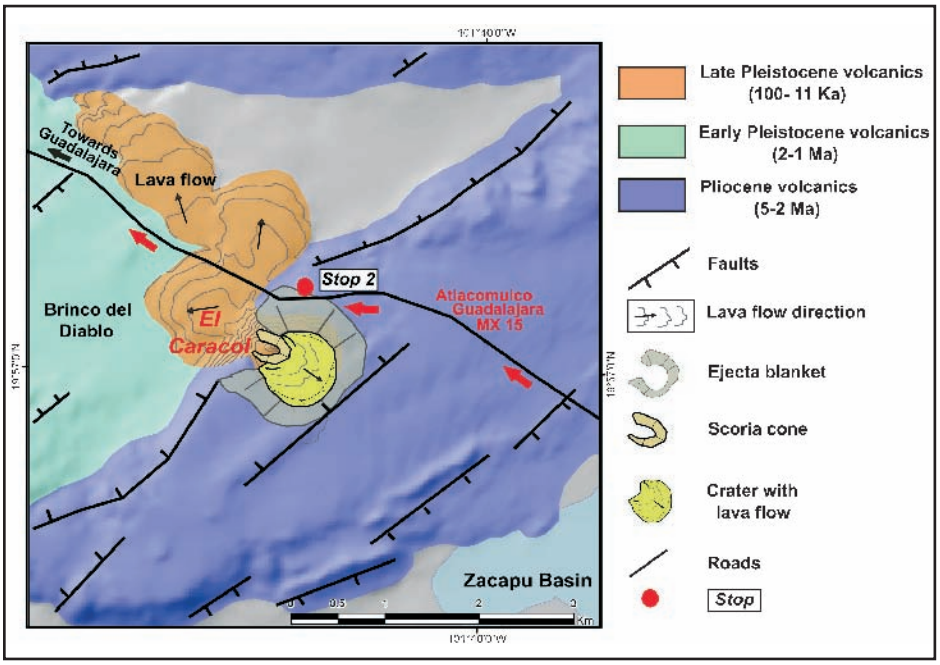

Figure 9: Simplified geologic map of El Caracol tuff cone and associated scoria cone and lava flows showing the location of Stop 2. For location see also map in Fig. 4.

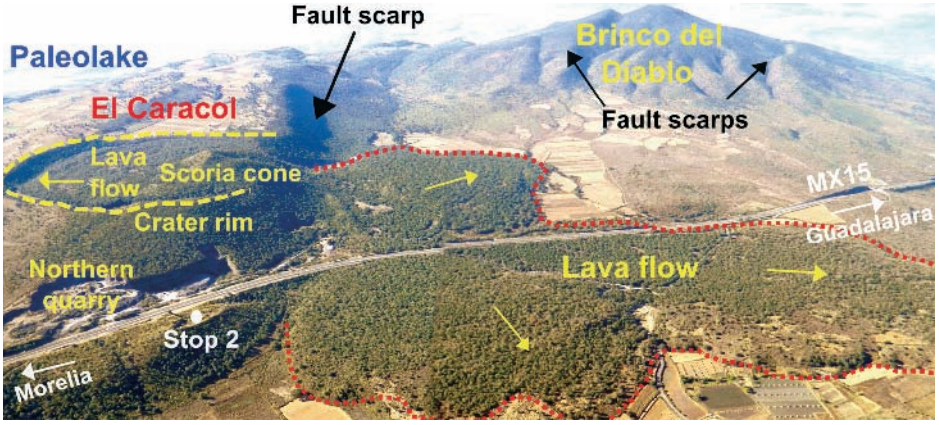

Figure 10: Aerial view from the NNE of El Caracol tuff cone located to the north of Zacapu paleo-lake. Note unusual location of El Caracol on top of a small tectonic horst (normal faults are indicated by black arrows). At the end of the El Caracol eruption a small scoria cone formed near the NW rim of the tuff cone crater producing lava flows that first filled the crater and later spilled over its western rim (yellow arrows indicate flow direction). Large quarry (Stop 2) near freeway is also indicated. See also Figs. 4 and 8.

Figure 11: View from freeway towards large quarry (Stop 2) on the northern slope of El Caracol tuff cone. El Caracol phreato-magmatic deposits are best exposed at this location. See dredges for scale.

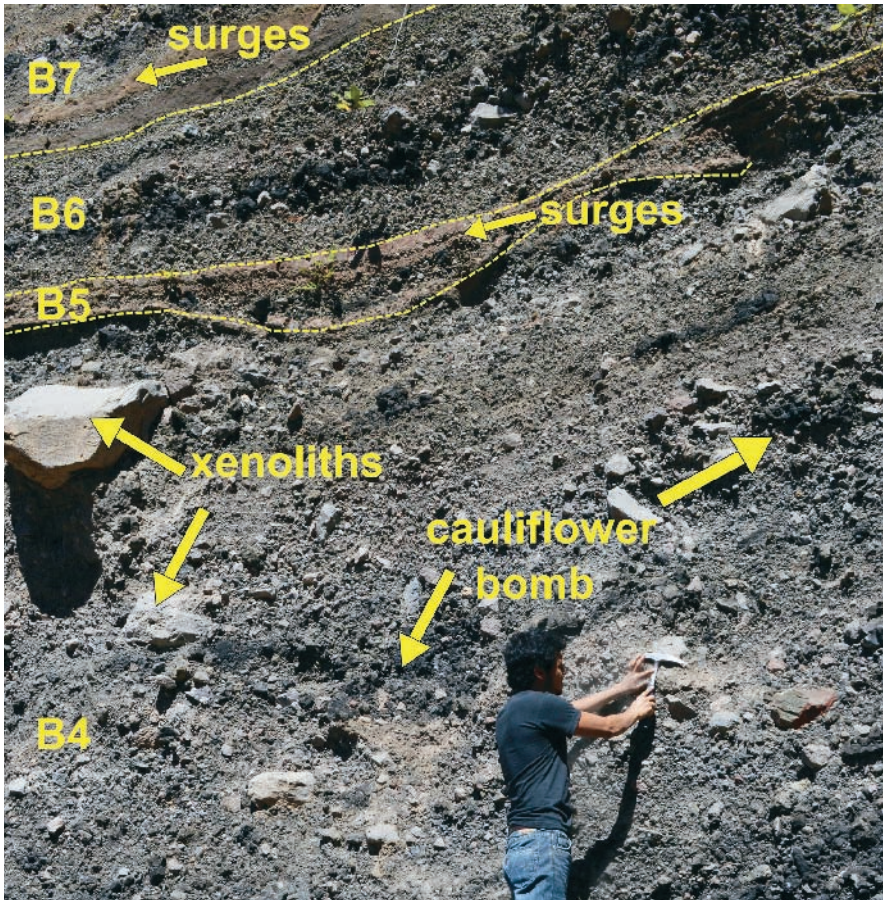

Figure 12: Close-up photo of proximal El Caracol phreato-magmatic deposits exposed at northern quarry (Stop 2).

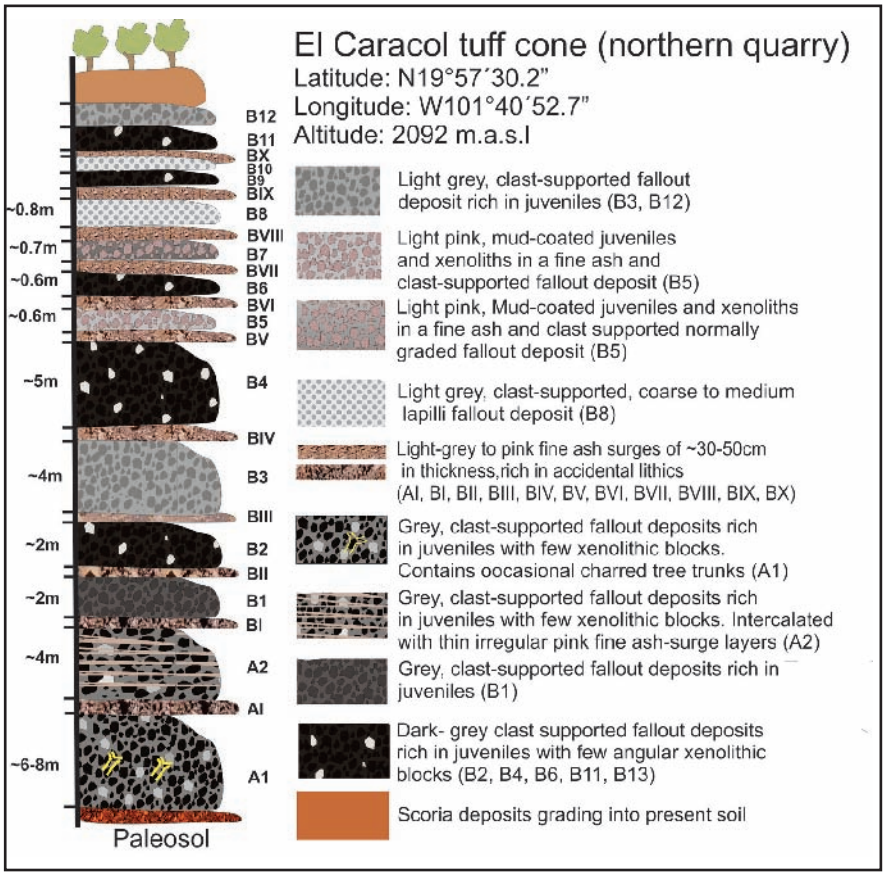

Figure 13: Stratigraphic sequence (mostly phreato-magmatic surge-and-fallout deposits) of El Caracol tuff cone exposed at northern quarry (Stop 2) near freeway No. 15.

niles (cauliflower bombs) along with a few angular xenoliths (andesite and basaltic andesite). Also present are surge deposits intercalated as thin indurated stratified layers of fine ash bearing mud coated clasts. In comparison to Alberca de Guadalupe, the entire sequence indicates much less water involved during the eruption process.

Stop 3: Canal at Villa Jiménez (19°55'12.57", 101°44'48.28"1992 m)

En-route to Alberca de Los Espinos we cross the canal of Villa Jiménez (Fig. 14). This canal was initially excavated at the end of the 19th century at the topographically lowest point of the northeastern Zacapu lake shore. Only during unusually rainy years the water level of the shallow lake would be high enough to overspill at this site and empty into the Río Angulo to the north. This observation encouraged greedy owners of nearby haciendas to dig a canal to drain the entire lake to gain an enormous area of new arable land and, at the same time, eliminating marshy areas considered to be unhealthy. This endeavour took several years and culminated in 1902 (Reyes-García and Gougeon, 1991). As a result, the ecology and economy of the region changed abruptly. Previous lacustrine and riparian habitats disappeared quite suddenly and the native population (mostly Purhépecha Indians) that had inhabited towns and hamlets at the margin of the lake and had spent for generations part of their lives on canooes fishing, hunting water foul, etc. had to adapt quickly to an unforseen situation that was imposed on them quite arbitrarily in the name of modernity. Today, the main crops grown in the basin include corn and sorghum.

The canal observable today has been refurbished on several occasions and still serves as an outlet for the Zacapu basin. It connects to the Río Angulo which flows north to the Río Lerma, the main river draining western-central Mexico into the Pacific.

Stop 4 (A, B, C): Alberca de Los Espinos: A phreatomagmatic tuff cone that obstructed the former outlet of Zacapu lake and changed the environment

Stop 4A: Crater rim (19°54'19.33", 101°45'57.79", 2045 m)

After passing the Canal of Villa Jiménez, arrive at the southern slope of the geologically significant Alberca de Los Espinos

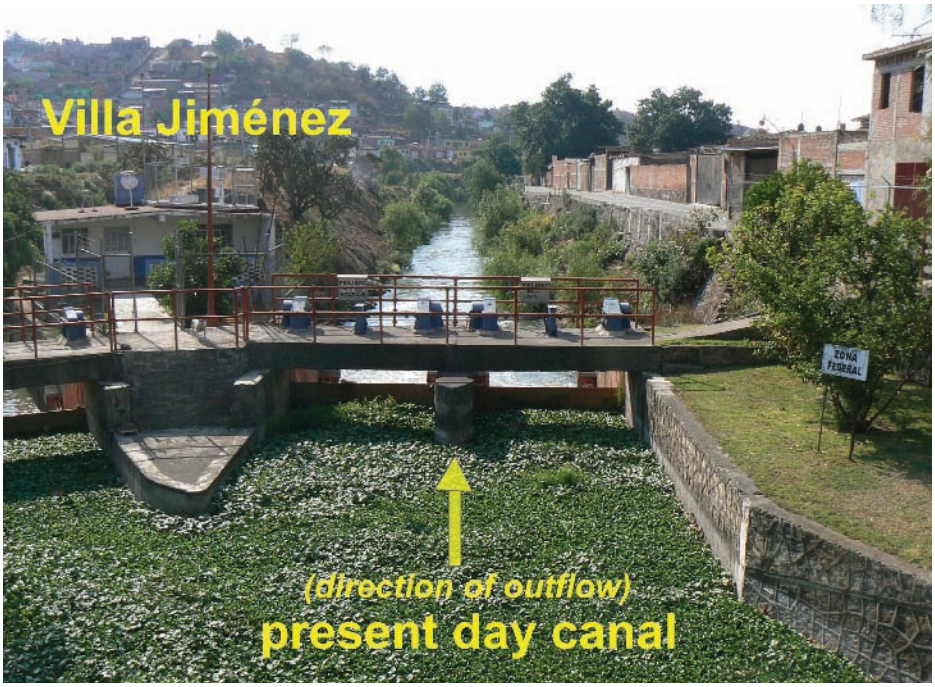

Figure 14: Canal at Villa Jiménez (Stop 3) that served for draining Zacapu lake more than 100 years ago (direction of the outflow is indicated by arrow).

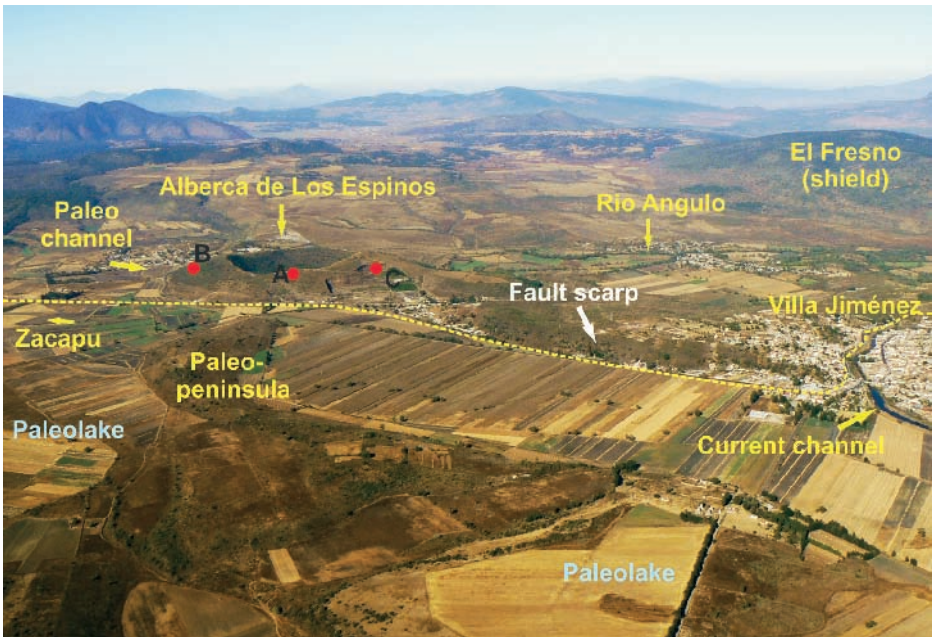

Figure 15: Aerial view toward the NNW of Alberca de Los Espinos tuff cone and canal at Villa Jiménez. The eruption of the tuff cone occurred at the location of the former natural outlet of the Zacapu paleolake obstructing the outflow. As a result, the level of the lake rose several meters until it could spill over at the location of the present canal of Villa Jiménez (see also Fig. 16). A, B, C (see text) denote places to be visited at Stop 4.

phreatomagmatic tuff cone located at the NW margin of the Zacapu tectonic lacustrine basin (Figs. 4, 15, 16). From here, climb on foot to the crater rim (Stop 4A) to enjoy a panoramic view of the crater and better understand the surrounding landscape, which includes the Malpaís Prieto, the youngest lava flow in the region (see also photos at inner front cover). The highest point of the crater rim (2100 masl) rises ~110 m above the ground of the lacustrine plains to the SE. The crater has an NE-SW oriented elliptical shape and a maximum diameter of 740 m. Its interior is occupied by a maar lake that has a maximum diameter of 350 m and reaches a maximum depth of 29 m below its present surface at 1980 masl. The tuff cone has an average basal diameter of 1200 m and surge deposits are preserved as far as 2 km from the present crater rim. The maximum elongation axis of the crater is parallel to a regional fault trending NE-SW that runs through the cone dropping the SE block (Fig. 16). Remnants of an old pre-existing scoria cone are exposed on the NE inner walls of the crater, as evidenced by cliff-forming lava flows topped by layers of spatter agglutinate.

The occurrence of a phreatomagmatic volcano such as Alberca de los Espinos at the northern limit of a lacustrine basin is not surprising. What makes this volcano special is its exact location at the former outlet of the Zacapu lake (Siebe et al., 2012). As a result of the eruption, the outlet became sealed and the water table of the lake rose several meters, before a topographic low near Villa Jiménez (present location of the canal) situated 2 km to the NE of Alberca de los Espinos, could serve as a new outlet reconnecting the basin with the drainage of the Lerma river to the north. As a result of the lake level rise, the surface area of the lake increased by ~30% from ~205 to ~310 km^2. Hence, the Zacapu lake deposit sequence potentially records a significant transgression after the timing of this short-lived monogenetic eruption.

Several of the large quarries at the outer slopes of the tuff cone expose clean contacts with the underlying paleosol. Samples from this paleosol obtained at different quarries yielded radiocarbon dates of around 25,000 yr. BP. This age is of importance because it not only dates the eruption, but indirectly also dates a major lake transgression and in consequence an important environmental change which in this case was not controlled by climate (e.g. changes in temperature and precipitation), but by endogenous forces (those forces that also created the fault-controlled lacustrine basin surrounded by volcanoes in the first place). Hence, the formation of this tuff cone subsequently led to the expansion of a habitat hosting numerous aquatic and riparian plant and animal communities that attracted nomadic early humans and promoted the development of agriculture in this area as evidenced by the numerous pre-Hispanic archaeological sites discovered nearby (e.g. Arnauld et al., 1994).

In order to better understand the environmental factors that fostered the rise of early human civilization in this region, palaeo-climate studies focusing on the analysis of the lake sediments (and particularly on their microfossil contents) have been carried out (e.g. Metcalfe, 1992). Although particular attention has been paid to the Holocene, some of these records go back

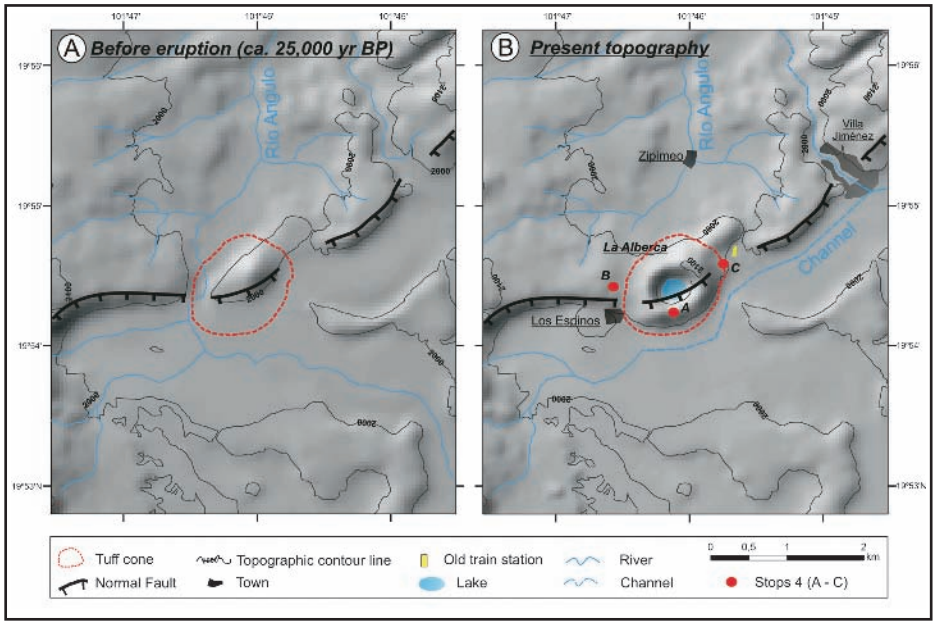

Figure 16: Topography of the Alberca de los Espinos area before and after the eruption of the tuff cone ~25,000 years ago. Note that the drainage pattern of the Río Angulo changed significantly as a result of the eruption (see also Fig. 15). A, B, C (see text) denote places to be visited at Stop 4.

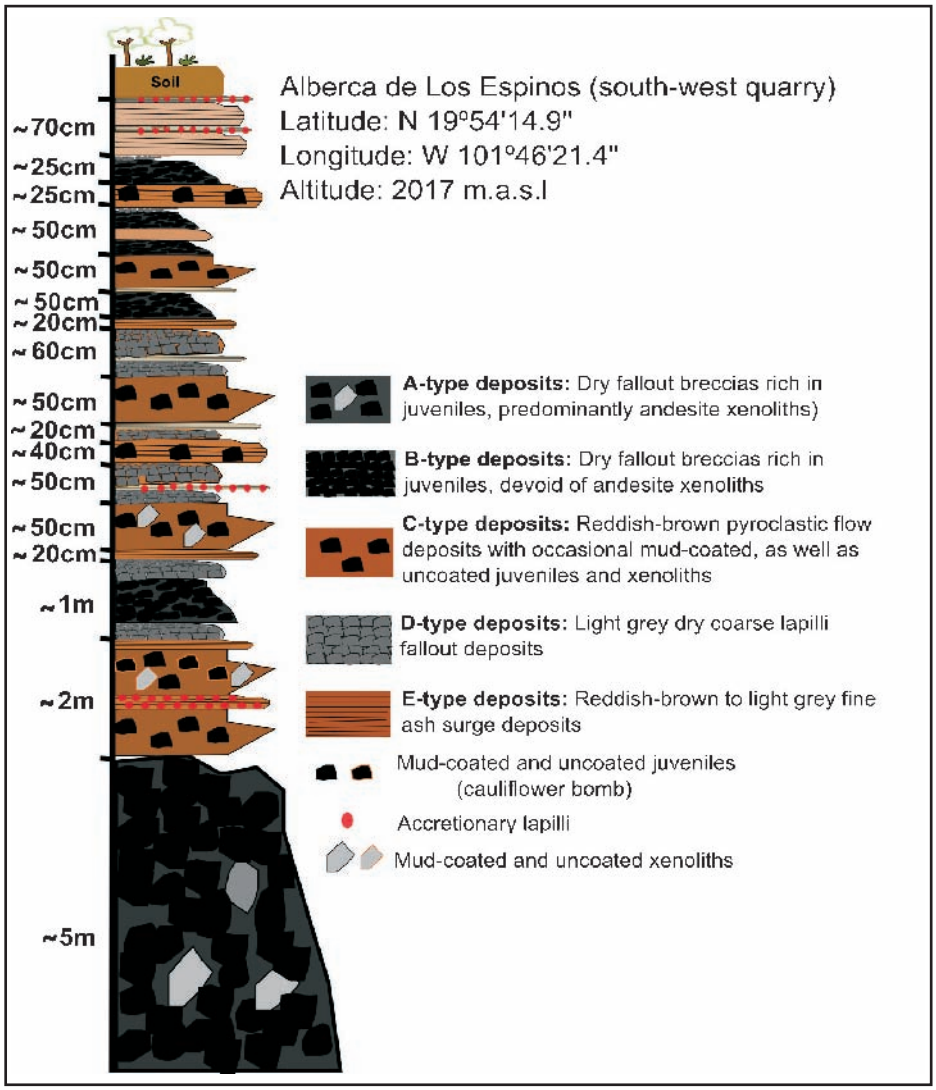

Figure 17: Stratigraphic sequence (mostly phreatomagmatic surge-and-fallout deposits) of Alberca de Los Espinos tuff cone exposed at SW quarry (Stop 4B).

as far as 52,000 yr. BP (e.g. Tricart, 1992; Metcalfe and Harrison, 1984; Ortega et al., 2002). Interestingly enough, these studies (which include the analysis of lake sediment cores, up to 10 m in length) have identified a major discontinuity dated at 28,000-25,000 yr. BP. Interpretation by these authors in regard to the origin of this discontinuity varies (some interpret it to represent a regression or "hiatus", others mention a transgression of the lake) but all share a marked reluctance to come up with a clear-cut answer. As hinted above, we think that we have found the answer to the question of the nature of this discontinuity by dating the eruption of the Alberca de los Espinos tuff cone at 25,000 yr. BP. Our research shows that palaeoenvironmental studies of lake sequences need to consider not only climatic factors (which are admittedly important), but also tectonic and volcanic activity as potential variables controlling the level of the water table, which especially in the case of shallow lakes such as Zacapu, can have considerable ecological impact. In this context, it is worth mentioning that so far, we have been able to identify a total of 12 Late Pleistocene/Holocene (<25,000 yr. BP) monogenetic volcanoes within the catchment area (1480 km^2) of the Zacapu basin which has a perimeter of 230 km. Judging by the young morphology of the numerous NE-SW oriented extensional fault escarpments, and the occurrence of coeval lake deposits at different altitudes (vertical displacements of tens of meters), this area is certainly still seismically active. Hence, study of the lake deposits should not only consider volcanic eruptions, but also the occurrence of sudden catastrophic differential vertical movements of the lake floor.

Stops 4B and 4C: Proximal deposits of the tuff-cone at the W and NE quarry sections (4B: 19°54'14.78", 101°46'21.72"; 2016 m, and 4C: 19°54'34.51", 101°45'53.06"; 2069 m)

The deposits of this tuff-cone are superbly exposed at several quarry sections. Stops 4B and 4C show nearly complete sequences (Figs. 15, 16). The deposits are poorly sorted (Mdφ= -4.7 to 3.5, σφ= 1.38 to 3.88) and display several episodes of drier magmatic fallout units (rich in juveniles, SiO_2=57.6 wt%) alternating with fairly indurated wet phreatomagmatic surge (with accretionary lapilli) along with

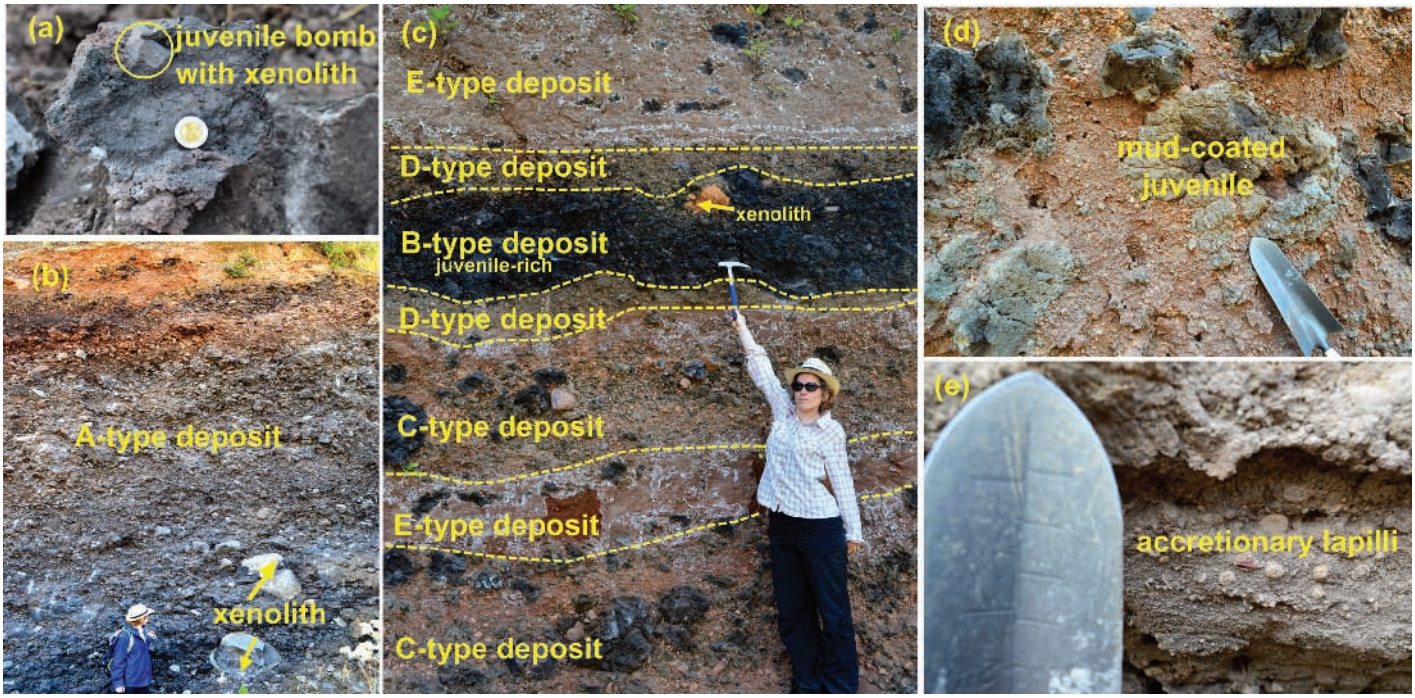

Figure 18: Photos displaying details of Alberca de los Espinos phreato-magmatic deposits at the SW quarry. The types of deposits are outlined in Fig. 17. a) Andesite xenolith in dark juvenile cauliflower-type clast from A-type deposit at the base of the startigraphic section (coin diameter=2 cm, for scale) b) A-type deposit: Clast-supported, juvenile-rich with few angular xenoliths (grey, vesicular and non-vesicular andesite fragments, containing micro-phenocrysts of plagioclase) indicating a drier magmatic episode. c) Alternating stack of different deposit types: B-type deposits are similar to the A-type, but devoid of xenoliths. C-type deposits were produced by pyroclastic flows (surges) and consist of mud-coated and non-coated juveniles and angular xenoliths embedded in fairly indurated, reddish-brown fine ash. D-type deposits consist of friable fallout units containing grey-colored, clast-supported, coarse lapilli, that are always present at the base and top of the B-type deposits, forming a symmetric arrangement. E-type deposits predominate in the upper part of the sequence and consist mainly of several thin units of fairly indurated, reddish-brown to gray, fine surge deposits stacked together bearing occasional accretionay lapilli. d) Mud-coated juveniles embedded in C-type deposits (small shovel for scale is 15 cm long). e) Accretionary lapilli in E-type deposits (small shovel for scale).

thick pyroclastic flow sequences (displaying mud-coated juveniles and lithics in a fine matrix). The deposits were classified into different types in order to decipher the eruptive history (Figs. 17, 18). At the northern quarry near the railroad tracks (not to be visited on this occasion), tree casts are evident in the lower pyroclastic-flow units, suggesting the existence of ample vegetation at the time of the eruption.

DAY 2: SCORIA CONES, DOMES, AND SHIELDS OF THE MESETA TARASCA (TARASCAN HIGHLANDS) BETWEEN ZACAPU AND URUAPAN AND COLONIAL TOWN-CHURCHES

During the morning of this day two of the hundreds of monogenetic scoria cones encountered in the MGVF will be visited. The first, Las Cabras (Stops 5 and 6) is located in the western periphery of the Zacapu basin (Figs. 2, 4). The second, Juanyan (Stop 7) is a nearly perfect cone further SW in the vicinity of Cherán (Figs. 24, 25). Then we will drive to the town of Paracho (Stop 8) and visit a nearby quarry displaying a block-and-ash fan (Stop 9) emplaced during the eruption of the Paracho dome (also called Cerro El Águila), the highest peak (3330 masl) in the area (Figs. 24, 25). In the town of Pomacuarán we will have lunch and visit an ancient church with adjacent *guatápera* (hospital) dating back to early colonial times (Stop 10). If time allows, we will continue to Nurio (Stop 11) and Cocucho (Stop 12), where further architectural gems (churches with *guatáperas*) will be visited before driving via Angahuan and Capácuaro to Quinceo (Stop 13). From there we will have a view of "El Metate", the youngest mid-volume volcano (dome or shield?) of the entire MGVF. The night will be spent in Uruapan at Hotel Mansión del Cupatitzio.

Itinerary: Exit Zacapu and head west on highway No. 15 in direction of Carapan and Zamora (Fig. 4). Shortly, on the right side of the road, the dark grey Capaxtiro andesite lava flow field is encountered. Its age is unknown but should be <3,000 years judging by its young morphology (see also photo on inner back cover). The Aa-type flows are almost devoid of vegetation and display steep flow fronts that are 30 m high. After 10 km (~30 Mins.), shortly before reaching the small village of Eréndira (Fig. 19), turn right on an unpaved road and continue few hundreds of meters towards a quarry (Stop 5). Here, one of the largest hummocks dotting the surface of the proximal lava flow field produced by Las Cabras breached scoria cone can be inspected. Later return to paved road and enter Eréndira. Turn right from the center of the village and follow another unpaved road for 3 km (~15 Mins.) to the NE until reaching an area of quarries located between the Las Cabras and Molcajete scoria cones (Fig. 19). One of these quarries (Stop 6A, see details below) displays the entire Las Cabras fallout sequence. Return to the paved road at Eréndira and drive west in the direction of Carapan for 1.5 km. Here turn right and follow the unpaved road for ~2 km (10 Mins.) and arrive at another quarry (Stop 6B) displaying 10 m of Las Cabras proximal scoria fallout deposits. After paying a visit to the quarry return to highway 15 and continue west to

Carapan and arrive at major road junction (Fig. 2). Here turn left (south) and drive towards Cherán (the entire stretch from Stop 6B to Cherán is ~50 km and takes about one hour). Shortly before arriving at Cherán (Figs. 24, 25) notice Juanyán scoria cone with a nearly ideal conical shape (Fig. 26). Drive further towards the town of Cherán and continue to its southern limit. Here turn right on paved road towards Paracho. After 2 km (shortly before reaching the Universidad Intercultural Indígena) turn right on unpaved road that after ~3 km (surrounding the SE sector of the Juanyán cone) leads to a large quarry on its eastern lower slope (Stop 7, Fig. 27). After inspecting proximal scoria fallout deposits return to paved road, continue for 10 km (15 Mins.) and arrive at the town of Paracho, famous for the manufacture of guitars. From here (Stop 8) you can obtain a good view of Paracho dome toward the SW (Fig. 29A). Pass through the town and exit for Uruapan. After ~2 km turn left, continue further for 300 m and arrive at a gravel-and-sand quarry pit (Stop 9) excavated into a block-and-ash fan at the NE slope of Paracho dome (Fig. 29B). Inspect the deposits. Return to paved road and turn left in the direction of Uruapan. After ~2 km (junction) turn right (NW) in direction of Cocucho and drive for ~3 km to arrive at Pomacuarán, a small village with a colonial church and guatápera (Stop 10, Fig. 30A), another good location to have lunch. After lunch drive NW for ~5 km and arrive at Nurio (Stop 11, Fig. 30B) and 6 km later at Cocucho (Stop 12, Fig. 31). Both towns host colonial churches with guatáperas. From Cocucho drive to Charapan (6 km), Corupo (3 km), Angahuan (7 km), San Lorenzo (11 km) and arrive at Capácuaro (6 km), another Tarascan village located at the foot of one of the El Metate dacite lava flows (Figs. 25, 32). Later, exit the village and drive NE for 6 km to arrive at Quinceo (Stop 13), where a good view of El Metate can be obtained. From Quinceo drive to hotel "Mansión del Cupatitzio" in Uruapan (23 km, 30 Mins.).

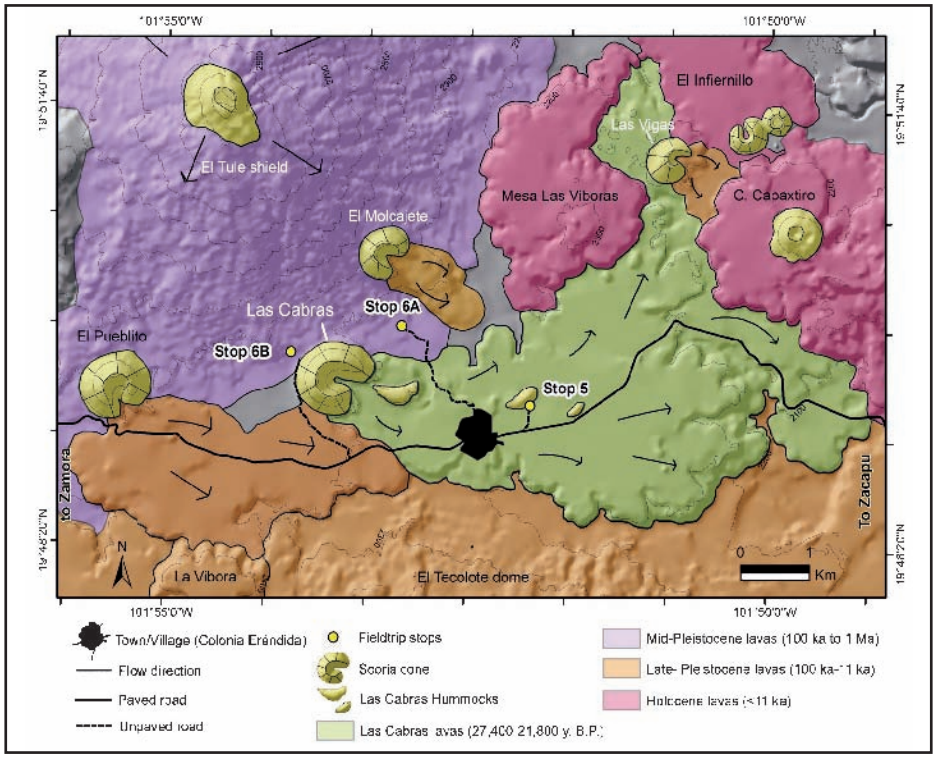

Figure 19: Geological sketch map of Las Cabras cone and associated lava flows indicating location of Stops 5 (hummock) and 6A and 6B (fallout deposits).

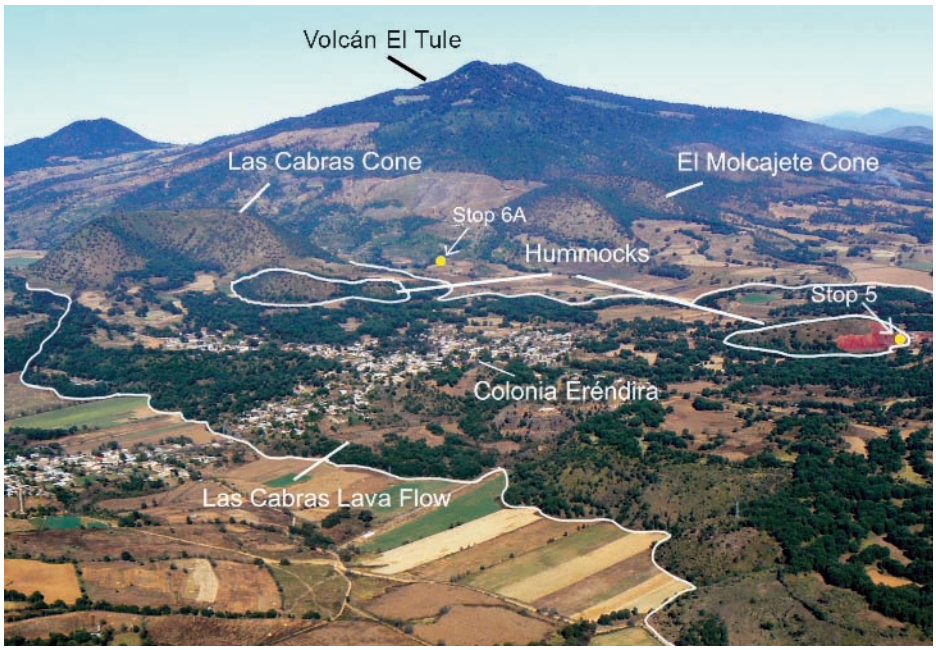

Figure 20: Aerial photograph of Las Cabras scoria cone and proximal deposits (hummocks, thick andesite lava flows). Note red color of scoria agglutinates exposed in quarry of hummock to the right (Stop 5). Photo taken from the southeast.

Stops 5 and 6: Las Cabras breached scoria cone

The Las Cabras scoria cone is located 10.5 km west of the Zacapu lacustrine plain in a tributary valley between two older volcanoes: The steep Late Pleistocene Cerro El Tecolote dome and the older (~0.11 Ma) Cerro El Tule basaltic-andesite shield. The latter shares the typical circular geometry and low-sloping flanks of other shields in the MGVF (Figs. 4, 19, 20). Although Las Cabras volcano is morphologically similar to many other young scoria cones in this area, its products display peculiar sedimentary and textural features that make it particularly interesting.

The eruption of the volcano included two main phases of activity: An explosive phase that built a ~300 m high scoria cone and deposited thick ash-fallout exposed mainly to the north and northwest of the cone, and an effusive phase that formed a >7 km long lava flow field that emerged from a major breach in the cone (Figs. 19, 20). The area covered by the flows and their volume were estimated at 18.2 km^2 and 0.6 km^3 respectively, while the volume of the cone is only 0.06 km^3. Radiocarbon

dating of paleosols (4 samples) directly below the fallout deposits yielded ages ranging between 27,400 and 21,800 yr. B.P.

The composition of the erupted products ranges from basaltic-andesite to andesite, with scoria clasts spreading a slightly wider range towards more silicic compositions (56.4–63.0 SiO_2 wt.%) than lavas (56.9–60.4 SiO_2 wt.%). The mineralogy is similar for lava and scoria samples: Both contain olivine and plagioclase phenocrysts (<1-3 mm) in a matrix rich in plagioclase microlites. Olivine is the dominant phenocryst phase (25 vol.% in lava, 30 vol.% in scoria) with plagioclase accounting for 15 vol.% in lava and 20 vol.% in scoria.

Stop 5: Large hummock with coarsely stratified deposits rich in bread-crust bombs (19°19'25.8", 101°51'58.5", 2252 m)

The lava surface displays a few peculiar elongated mounds or hummocks (Figs. 19, 20). This quarry exposes the interior of the second largest hummock (420 m long, 200 m wide, 15 m high), revealing coarsely stratified, partly-welded fallout products rich in scoriaceous spatter-bombs and large bread-crust bombs (~1-2.5 m in size) (Fig. 21). The bombs have been piled up on site due to their non-utility for road construction and hence are particularly well exposed at this location. They nicely display internal concentric vesicular zoning and stretched and cracked outer glassy skins (bread-crust surface textures).

These features are typical for proximal andesite scoria cone deposits, hence the hummocks must have originally been part of the cone. The hummocks probably formed as a result of the breaching of the eastern flank of the cone by the lava flow that then rafted parts of the detached cone down the flow. The elongation of the hummocks in the direction of the flow (Fig. 19) suggests that after detachment from the cone, these were carried on top of the lava flow.

Stops 6A and 6B: Quarries displaying fallout deposits with evidence for syn-eruptive rain and magma mingling (6A: 19°50'00.2", 101°53'10.5", 2265 m asl; 6B: 19°49'47.0", 101°53'51.7", 2324 m)

Proximal tephra fallout deposits at Las Cabras can be divided into three main parts: a) A basal indurated part dominated by thin fine-grained (ash and fine lapilli)

Figure 21: Exposure of the interior of a hummock at Stop 5 showing coarsely stratified deposits rich in bread-crust bombs. The largest bombs were left behind by quarrying activities forming piles at the base of the hummock. Photo taken January 29, 2014.

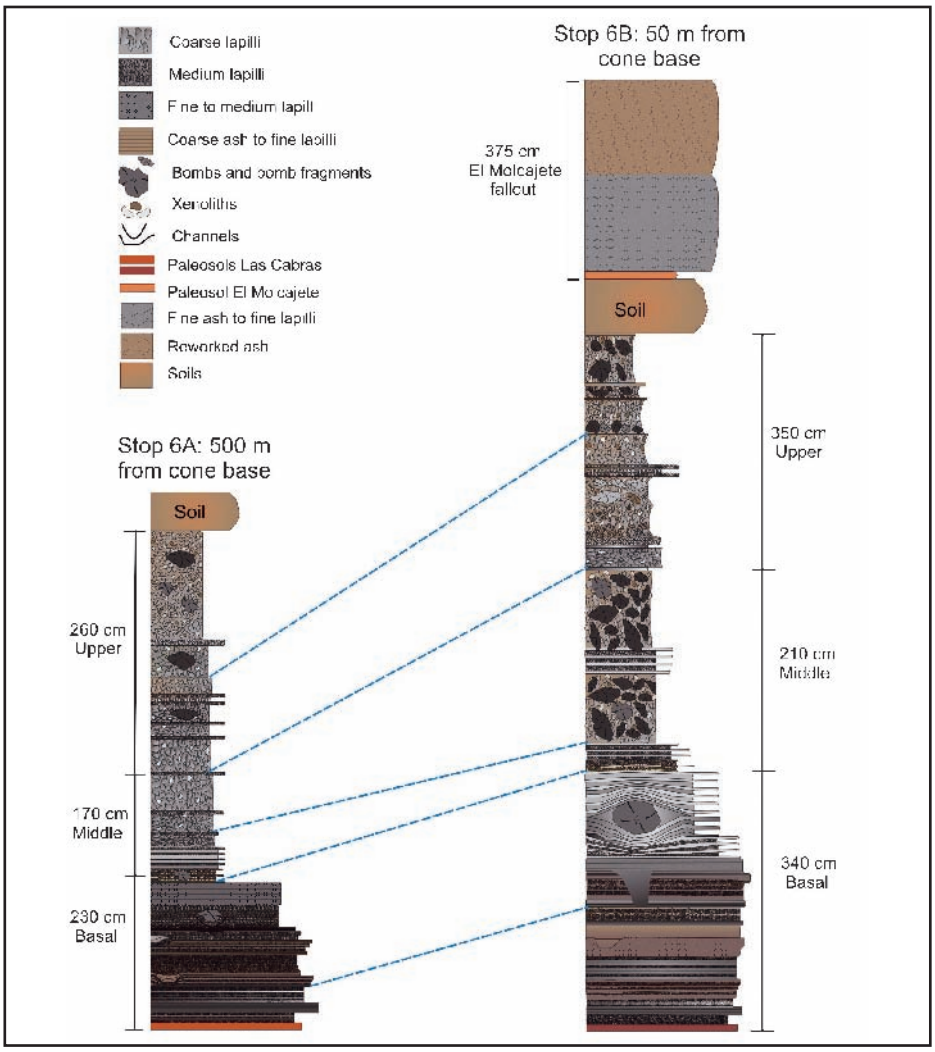

Figure 22: Stratigraphic sections of Las Cabras fallout deposits at Stop 6A located 500 m and another quarry (Stop 6B) located 50 m from the base of the cone. The different parts of the sequence (basal, middle, upper) described in the text are indicated. Layers at the most proximal quarry are thicker, richer in bombs, and contain larger bombs in the upper part.

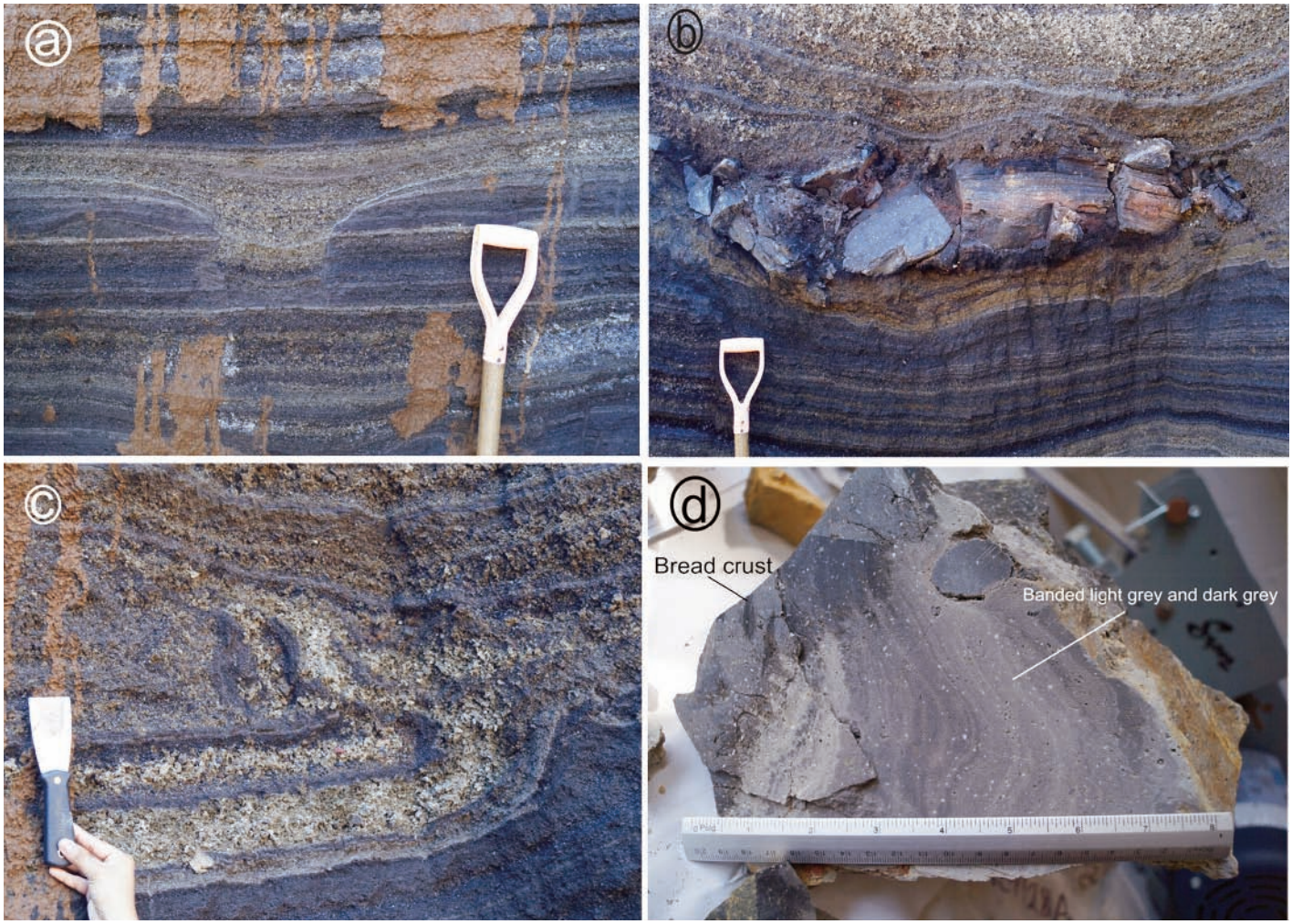

Figure 23: a) Erosion channels are 10-18 cm deep, 30-40 cm wide and affect mostly the finest and most indurated layers of the sequence (basal sequence at Stop 6A). b) Large bomb fragmented due to impact (2.11 m long, 0.43 m wide) observable in the basal part of the stratigraphic section (Stop 6A). c) Ductile deformation (folded layers) produced by ballistic impact (Stop 6A). d) Fragment of bread-crust bomb with outer dark glassy rind and distinct interior displaying parallel flow-banding. Layers of micro-vesicular light-grey material alternate with denser dark-grey layers. Larger xenolithic enclaves (<2 cm) surrounded by bands are common. All layers contain micro-phenocrysts of Plag (~2 mm), Ol (~1.5 mm), and biotite (~1 mm). The crust is richer in Plag than the core, but the core is richer in biotite (Stops 5 and 6).

layers and sporadic bombs, b) a middle part consisting of increasingly thicker (6-50 cm) and coarser grained (4-16 mm in size) layers, and c) an upper, friable part characterized by thick (10-100 cm) layers, coarse clasts (16-64 mm), and large bombs (Fig. 22). Layers forming the basal part consist of a mixture of highly-vesicular and dense juvenile clasts, while accidental lithics first appear in the middle and get more abundant toward the upper part, where juveniles are mostly of the highly-vesicular type.

Noteworthy at this location is the exposure of various sedimentary structures in the fine-grained basal part that are diagnostic of the occurrence of torrential rain during the eruption (Fig. 23). The most notorious are asymmetric erosion channels that are 10-18 cm deep, 30-40 cm wide, and display a near constant horizontal separation interval of 80-100 cm (Fig. 23a). They affect mostly the finest, most indurated layers of the sequence and are concentrated in two stratigraphic levels. Impact-sag structures that were produced by large bombs causing ductile and brittle deformation of the layers underneath (Figs. 23b, 23c) are also well exposed. In addition, bombs in the upper part of the sequence display peculiar characteristics. Many of them are dense and glassy, almost obisidian-like. Others show marked flow-banding (Fig. 23d) indicating mingling of two types of magma prior to explosive eruption. Interestingly, these peculiar bombs are petrographically distinct from the others since they bear phenocrysts of biotite (<4.1 mm), in addition to the usual olivine and plagioclase crystals.

Stop 7: Juanyan scoria cone (19°41'5.1"; 101°58'40.1"; 2220 m)

Juanyan scoria cone is located 2.5 km W of Cherán (Figs. 24, 25), where it stands isolated on the flat terrane of an intermontane valley surrounded by much older medium-sized volcanoes. Juanyan has been dated by the radiocarbon method at 9,000-10,000 yr. BP (Hasenaka and Carmichael, 1985) and has the most strikingly perfect conical shape (Fig. 26). Unfortunately, quarrying activities on its lower slopes have begun in recent years and might soon destroy its ideal symmetry. The largest quarry is located at the eastern base of the cone where typical proximal scoria fallout deposits are exemplarily displayed (Stop 7, Fig. 27).

The cone (2374 masl) rises 186 m above surrounding ground and is in many respects a typical representative for a Strombolian monogenetic volcano. But contrary to most other cones of this type in central Mexico, Juanyan did not produce lava flows. Its basal diameter is 0.94 km, the crater diameter is 0.34 km, and the volume of the cone has been estimated at

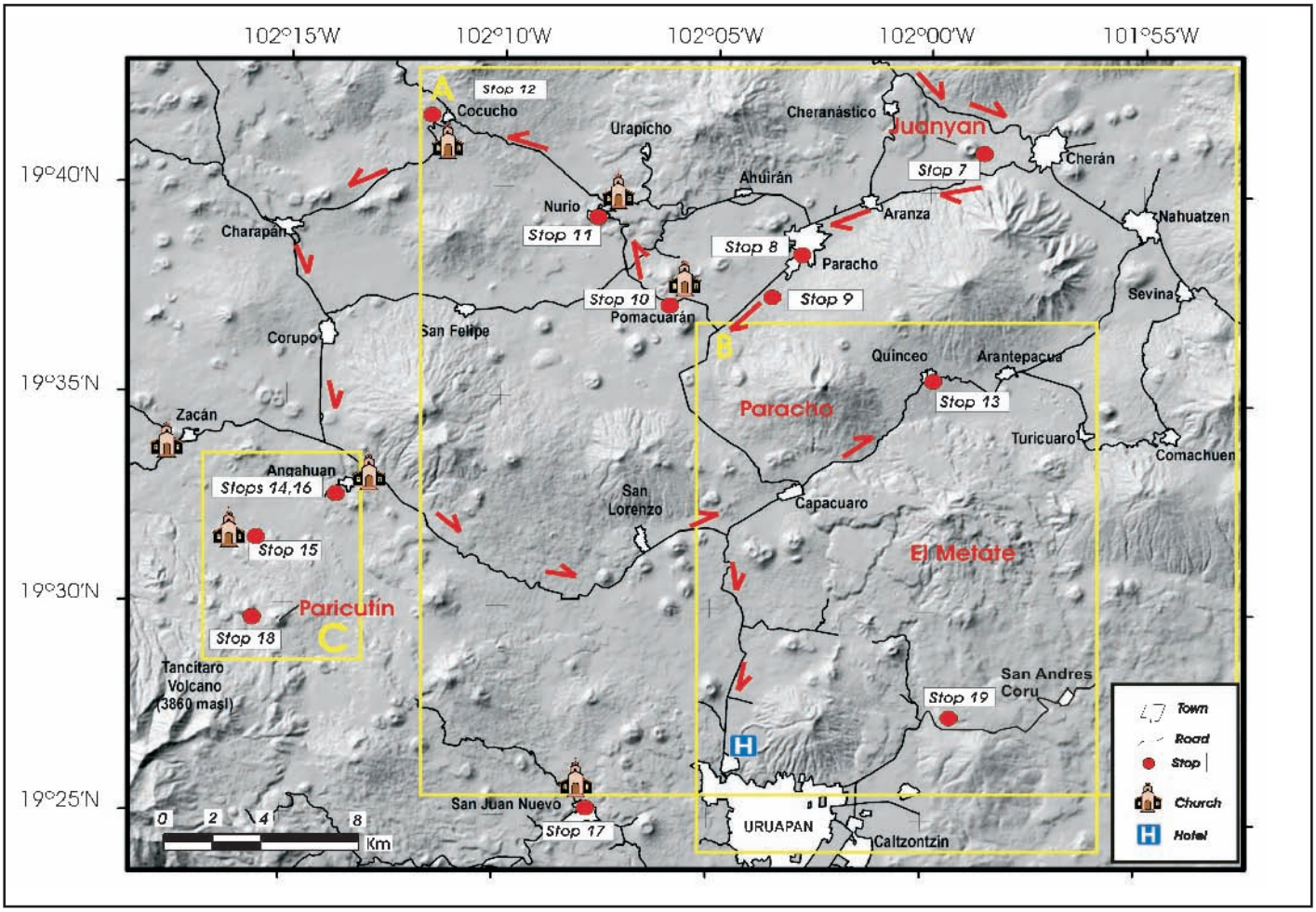

Figure 24: Digital elevation model of the Cherán-Paracho-Paricutin area showing travel route (red arrows) and Stops 7 to 19 to be visited during the second part of the excursion. Yellow rectangles A, B, and C denote areas covered by detailed maps in Figs. 25, 32, and 36 respectively.

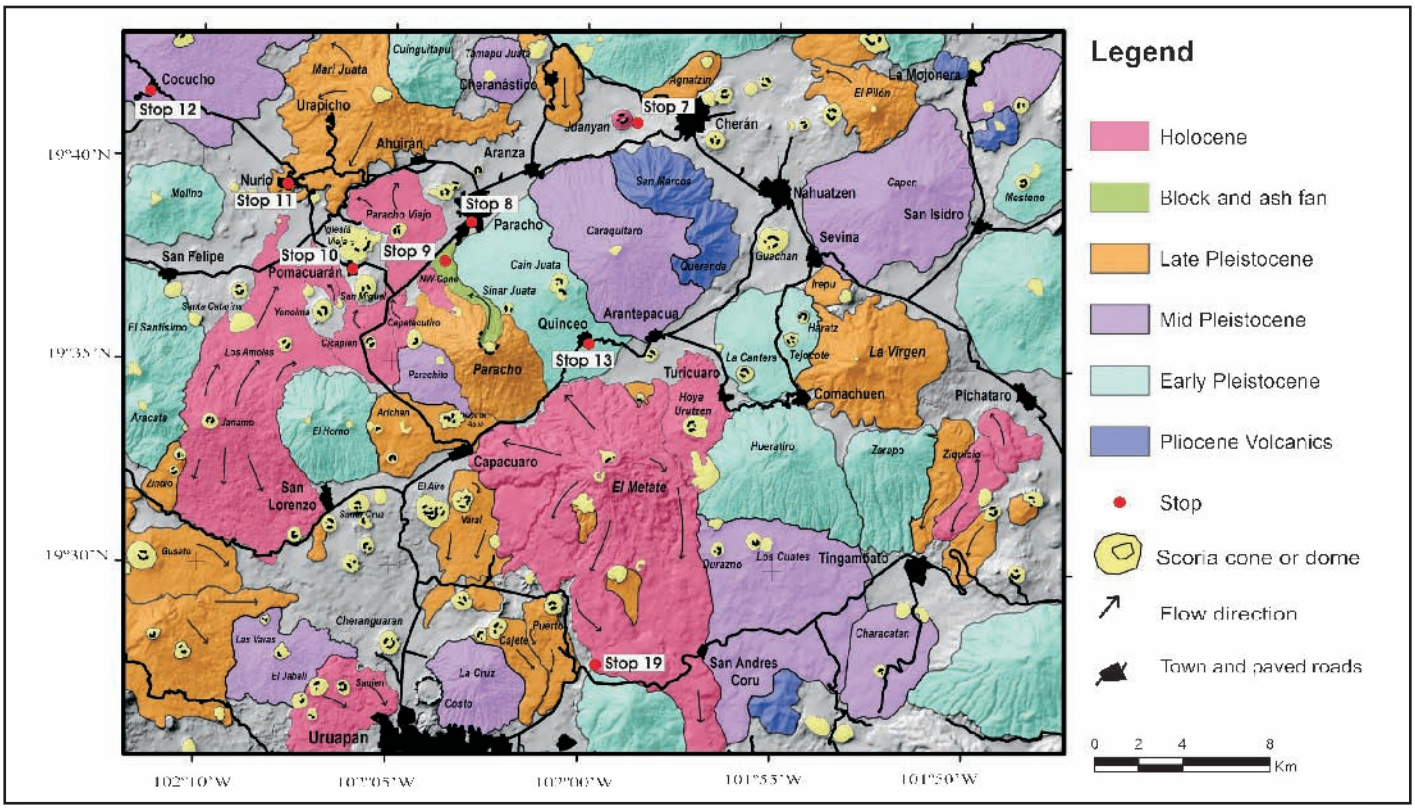

Figure 25: Simplified geologic map of the Paracho-Cherán area (Stops 7-13) to be visited during the 2nd day of the excursión.

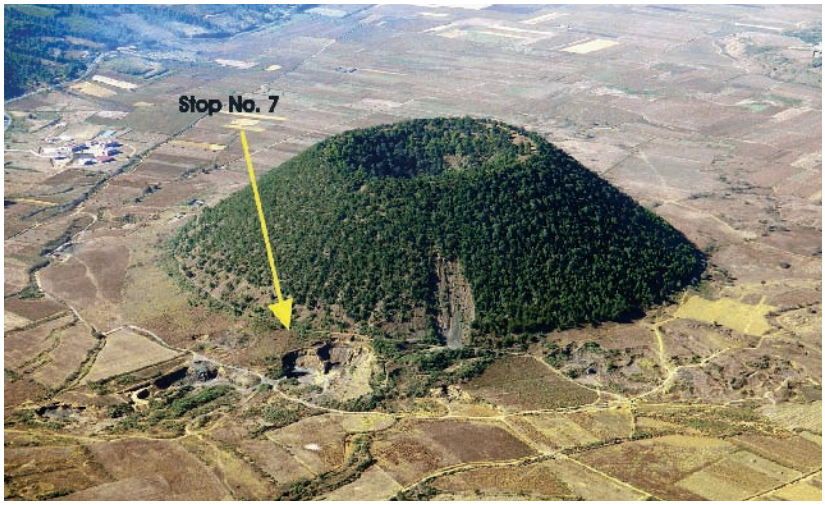

Figure 26: Aerial view from the NE of the nearly ideally shaped Juanyan scoria cone radiocarbon-dated at ~10,000 yr. BP. Arrow points at quarry (Stop 7).

Figure 27: Quarry at the NE slope of Juanyan scoria cone (Stop 7) displaying proximal scoria fallout deposits.

~0.07 km³. The volume of the medial and distal well-bedded ash-fallout is unknown, but might include a significant portion of the total volume since this layer has been identified at considerable distances from the vent (>10 km). The stratigraphic sequence (Fig. 28) displayed at the quarry consists of ~15 m of well-bedded, clast-supported, normally-graded alternating layers of ash to lapilli (Inman parameters: Mdφ=1.8; σφ=1.3), with occasional dense bread-crust bombs and ballistic angular lava blocks often associated with impact sags. Several layers display inverse grading caused by sliding (self-sieving) of the loose material on the oversteepened slope of the cone. The sequence indicates that the eruption was pulsating (violent-Strombolian) with the rise of multiple several-km-high eruption columns at the beginning and that explosions became weaker (Strombolian) toward the end of the activity.

The composition of the eruptive products is basaltic-andesitic (SiO_2=54 wt.%) with olivine phenocrysts in a glassy matrix rich in feldspar microlites and minor pyroxene grains. The olivines frequently show embayments and contain chrome-spinel. The lack of plagioclase and pyroxene phenocrysts and violent style of the activity indicate that the magma feeding the eruption was water-rich and probably ascended quickly without major periods of stagnation before reaching the surface.

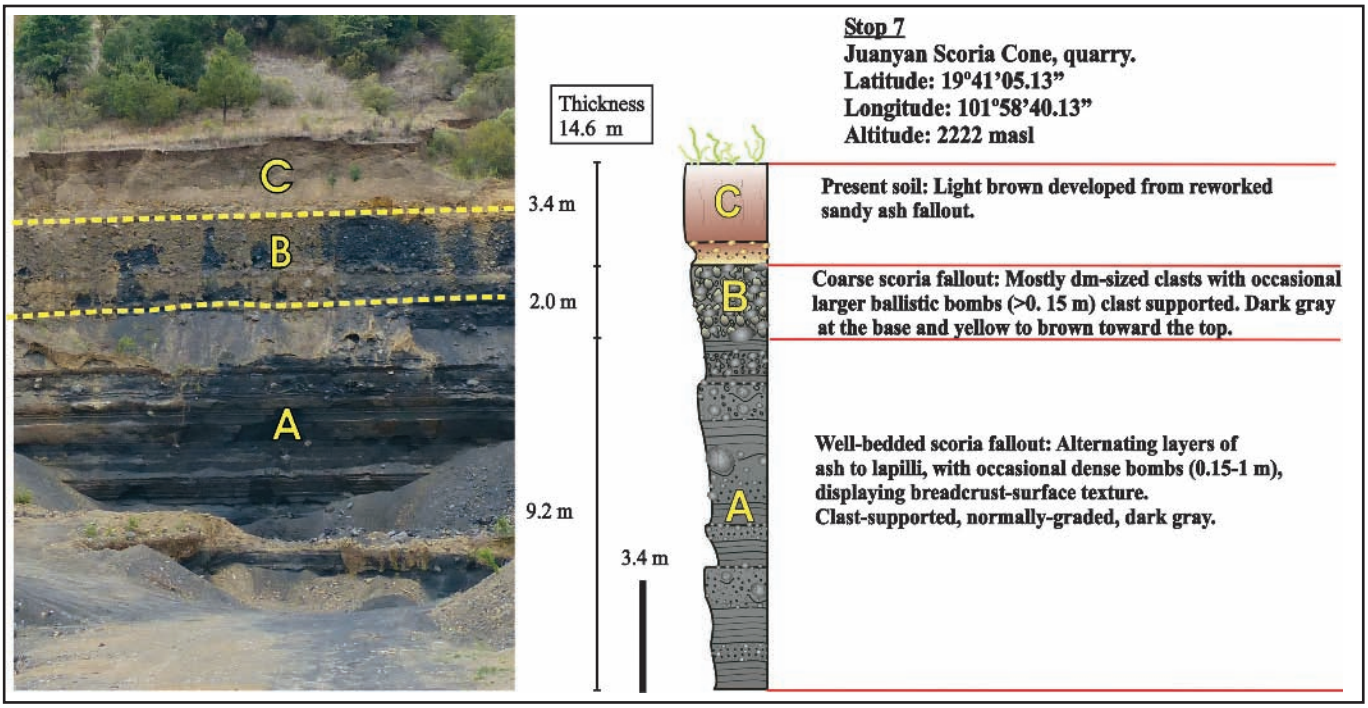

Figure 28: Stratigraphic sequence (proximal Strombolian fallout) at quarry of Juanyan cone (Stop 7).

Figure 29: a) View of Cerro Paracho from the town of Paracho (Stop 8). Note the steep walls of the protruding summit dome nested in a cirque from which a deeply incised dissected valley originates. The slope of the older neighboring Cain Juata shield is in the foreground. b) Block-and-ash fan (pyroclastic flow and lahar deposits) displayed at quarry (Stop 9) with Paracho summit dome in the background. c) Hollow tree-cast in the block-and-ash fan deposits at Stop 9. Notice oval shape of cast, probably produced by load of overlying deposits.

Stop 8: View of Cerro Paracho dome from the town of Paracho (19°3"28.0"; 102° 03'02.4"; 2238 m)

From the SW outskirts of the town of Paracho a panoramic view of Cerro Paracho (3340 masl) is accessible. Paracho is the highest volcano in this area and stands mostly isolated above its surroundings, with the exception of its NE flank that connects to a chain of NE-SW oriented older (Pliocene-Pleistocene) shields (Figs. 24, 25, 30). With a basal diameter of 6 to 8 km covering an area of 21.3 km^2, a height of 900 m above surrounding ground, and an estimated volume of 3.5 km^3, Paracho can be classified as a medium-sized volcano. Considering its slope angles (12°-16°) it could be catalogued more precisely as a shield-type volcano, ranging between the "Icelandic" and the "Galapagos" categories, according to the classification of Whitford-Stark (1975). However, whether this volcano should be really labeled as a shield is debatable (see below).

The most striking characteristic of Cerro Paracho is its steep protruding summit dome (Fig. 29a) emplaced inside a cirque from which a deeply incised valley originates. This valley drains the northeastern slope and connects to a wide block-and-ash fan (Stop 9, Figs. 24, 25, 30) that forms the substrate of the inclined plain to the north of Paracho.

Stop 9: Paracho block-and-ash fan (19°37'27.6"; 102° 03'41.0"; 2307 m)

This large quarry exposes up to 20 m of stratified deposits that form a block-and-ash fan at the foot (break in slope) of Cerro Paracho dome (Figs. 29b, 30). The deposits are coarse, crudely stratified, semi-friable, and consist mostly of dense-to-moderately vesicular, greyish, angular to sub-angular, juvenile andesite blocks in a medium-to-coarse ash-matrix of the same composition. The layers vary in thickness (several dm) and lack erosional unconformities or

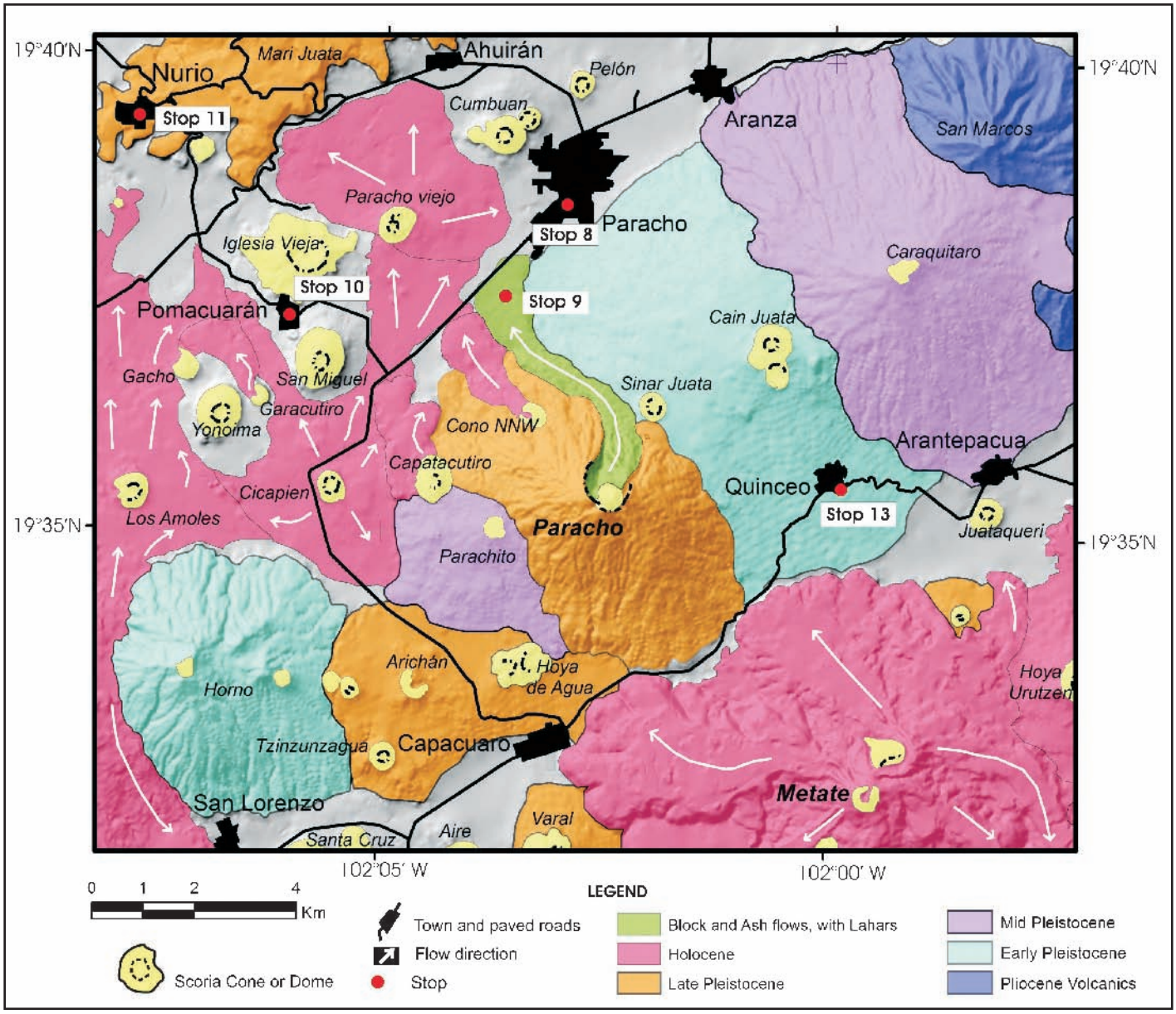

Figure 30: Simplified geologic map of the Cerro Paracho area (Stops 8-11, 13) to be visited during the 2nd day of the excursion.

paleosols between them indicating that the entire fan was built over a relatively short span of time (months to years). Charcoal fragments were not found within the deposits. Instead, horizontal cylindrical casts of large tree trunks are observable (Fig. 29c). We hypothesize that the fan originated during and shortly after the emplacement of the summit dome that crowns the Paracho edifice. Over-steepening of the viscous dome during growth led to its sequential collapse and the generation of multiple gravity-driven pyroclastic block-and-ash flows that were not hot enough to charcoalize engulfed vegetation. Subsequent removal of the pyroclastic deposits by lahars (following torrential rain) along the dissected valley led to the formation of the fan at the break in slope. The hollow tree casts were formed after deposition by the decay of the organic material over time. Hence, we believe that the fan consists primarily of lahar deposits.

A soil sample collected by us from the uppermost part of the clayey, thick paleosol directly underlying the block-and-ash fan sequence yielded an age of ~12,300 yr. BP. This age is in strong contrast to the K-Ar age obtained from lava on the flank of Paracho that was dated at 0.06±0.01 Ma by Ban et al. (1992). The age discrepancy strongly suggests that Paracho might be rather classified as a composite dome than as a monogenetic shield. The varying morphology and differences in the degree of preservation of some of the lava flow surfaces observable at Paracho's flanks also point toward multiple eruptions separated by geologically significant time spans. Paracho's products are quite homogeneous and consist mostly of andesitic lavas (SiO_2=61 wt.%) that are seriate-porphyritic to glomeroporphyritic (crystal-clusters of up to 5 mm) including intergrown plagioclase and pyroxene. Oscillatory-zoned tabular plagioclase phenocrysts are abundant and frequently show sieve-textures. Orthopyroxene is more abundant than clinopyroxene and the groundmass is hypocrystalline to microlite-rich.

Stop 10: Pomacuarán church and hospital (*guatápera*) (19°37'22.3"; 102° 06'13.2"; 2235 m)

After the military Spanish conquest (1519-1521) of Mexico by Hernán Cortés, a political and religious reorganization of un-

Figure 31: a) 16th century facade of hospital chapel at San Miguel Pomacuarán (Stop 10). b) Painted interior wooden ceiling (*artesonado*) of Nurio's main church dedicated to Santiago Apóstol (St. James) (Stop 11).

precedented dimensions was implemented in the territories and would produce the viceroyalty of New Spain. The "spiritual conquest" (Warren, 1985) which implied the change of beliefs and customs was a fundamental part of this endeavour. Dispersed populations were invited (voluntarily or by force) to live in towns (*reducciones de indios*) and the Catholic faith was systematically introduced all over the country. In Michoacán, this occurred in the 16th century, under the impetus of Bishop Vasco de Quiroga and the fervor of Augustinian and Franciscan monks, who erected numerous missions. In the Tarascan highlands, hospitals (locally known as *guatáperas*) were built as essential adjuncts to the missions to serve the impoverished native Purhépecha Indians. Each hospital compound included a chapel, many of which still stand in varying degrees of preservation. As a result, modest but significant early architecture remains in several towns in this area until today (Artigas, 2001; 2010; Perry, 1997). These hospital chapels are generally humble in appearance and plain in their exterior ornament, but inside frequently lavishly decorated with impressive wooden ceilings and choirs, a feature almost unique to this part of Michoacán. Some of these ceilings are in poor condition, but few have been restored recently.

The hospital chapel (or *guatápera*) at San Miguel Pomacuarán (Fig. 31a), a small Indian village in the rural Tarascan highlands is particularly interesting. In the 1800s, the 16th century mission church of the town was destroyed by fire. Its carved stone doorway survived and was reassembled and attached to the entrance of the nearby hospital chapel, also an ancient building that may have even predated the mission church.

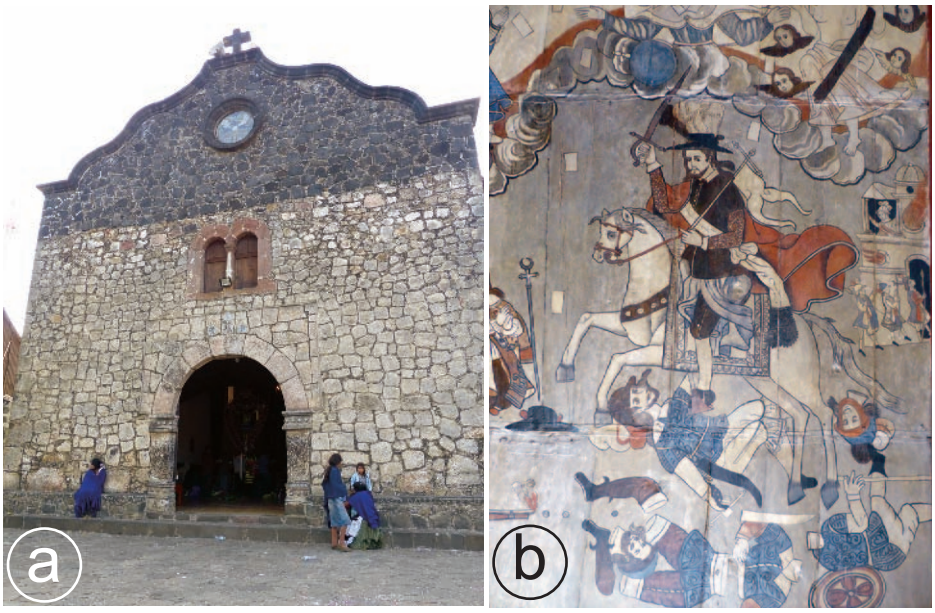

Figure 32: Town church of San Bartolomé Cocucho (Stop 12). a) Facade of church. b) Painted interior wooden ceiling (*artesonado*) depicting *Santiago Matamoros* at its central panel.

Preservation of the façade is a testament to local pride and continuity. Inside the chapel (which today serves as the town's parish church) is a wooden painted ceiling, one of the best preserved ceilings that are so unique to this region of Michoacán. The painted polychrome panels that conform the ceiling depict angels with scrolls, narrative scenes of saints and friars, biblical episodes, and prominent personalities in Christian church history.

Stop 11: Nurio mission church and "guatápera" (19°39'20.2"; 102° 07'49.1"; 2184 m)

Nurio's main church dedicated to *Santiago Apóstol* (St. James) and adjacent *guatápera* (hospital compound with chapel) is probably the best preserved example of its type in Michoacán. The main church displays a carved stone façade. Its interior is also spanned by a painted beamed ceiling (Fig. 31b) with ornate cartouches depicting colored angels while images of the Four Evangelists decorate the baptistry enclosure.

Behind the mission church, in a gated enclosure, is the *guatápera* compound. Before the chapel of *La Inmaculada Concepción* in the inner patio stands a yucca tree, that judging by its enormous size, must have a venerable age. Behind the simple façade of the chapel, the visitor is struck by a feast of vivid ornament and color: A beamed wooden ceiling (*artesonado*) is

painted with florid biblical figures and angels. A gilded altar and carved wooden door and choir complement the furnishings.

Stop 12: San Bartolomé Cocucho church (19°41'37.3"; 102°11'23.9"; 2427 m)

Another Franciscan mission church with a painted ceiling can be visited in San Bartolomé Cocucho. Behind a cold and massive stone-walled entrance (Fig. 32a), again a wooden ceiling can be admired inside the church. In this case the painted *artesonado* is limited to the section beneath the choir. The center panel depicts *Santiago Matamoros*, the warlike patron of the Spanish *Reconquista* or liberation of the Iberian peninsula from the Moors (Fig. 32b). This saint (Spanish incarnation of the Apostle James), whose bone relics are guarded in Santiago de Compostela (Galicia, NW Spain), also provided protection and spiritual guidance during the conquest-battles of Mexico, as evidenced by the outcome favouring again the victorious Spanish soldiers against the "heretics". Paradoxically, Santiago has been adopted in many Indian areas across Mexico (especially in the Tarascan highland) as a spiritual counter force to oppressive Spanish rule (quite a mysterious transmutation). Santiago is commonly portrayed in popular imagery mounted on a rearing horse and swinging his deadly sword against a turbanned enemy (in this case several enemies shown in different stages of dismemberment). In strong contrast, the flanking sections portray angels playing different musical instruments.

The network of missions established in the Tarascan highlands after the conquest did not only attend spiritual needs, but also engaged in practical matters of life. Each village was encouraged to specialize in a particular handcraft (e.g. textile weaving, wood-carving, etc.), some of which already existed in pre-Hispanic time. Many of these crafts still flourish today, as in Cocucho, a town specializing in tall clay jars known as *cocuchas*.

Stop 13: View of Cerro El Metate from Quinceo (19°35'38.6"; 101°59'42.6"; 2463 m)

From this locality an excellent panoramic view of El Metate (<3700 yr. BP, Hasenaka and Carmichael, 1985, 1986), the youngest mid-sized volcano of the MGVF, can be enjoyed. The edifice consists of well-preserved lava flows disposed radially around a summit dome (Figs. 33, 34). With a basal diameter of ~10 km and a height of ~600 m, El Metate displays a relatively flat profile (slopes of ~7°) resembling an "Iceland-type" shield according to the classification of Whitford-Stark (1975). But unlike typical shields that consist of numerous thin basaltic flows, El Metate produced only about 13 distinguishable A'a to blocky type andesite flows of an extraordinary thickness (up to 150 m). The high-aspect ratio flows reach distances from the summit that range between 3 and 15 km and cover a total area of 103 km^2. Individual flow volumes range between 0.5 and 3.5 km^3, adding up to a total of 11-15 km^3. Hence, the single volume of any of these lava flows is greater than the average volume of a typical monogenetic scoria cone.

Metate's composition is andesitic but not homogeneous (SiO_2=57-61 wt.%; MgO=2.8-5.2 wt.%). The most mafic lava was also the earliest to be erupted and is olivine-plagioclase porphyritic (<20 vol.%) with microphenocrysts of feldspar and orthopyroxene (<40 vol.%) in a dark hypocrystalline groundmass. Late lavas are seriate porphyritic (<55 vol.%) containing plagioclase, orthopyroxene, clinopyroxene, and elongated hornblende crystals in an hypocrystalline groundmass. Oscillatory-zoned tabular plagioclases are abundant and may show sieve textures. Reabsorption of hornblende into plagioclase+orthopyroxene+oxide+melt is evident under the microscope by the frequent observation of hornblende "ghosts".

Considering effusion rates of such high-viscosity lava flows and assuming sequential outpouring, we estimate that the

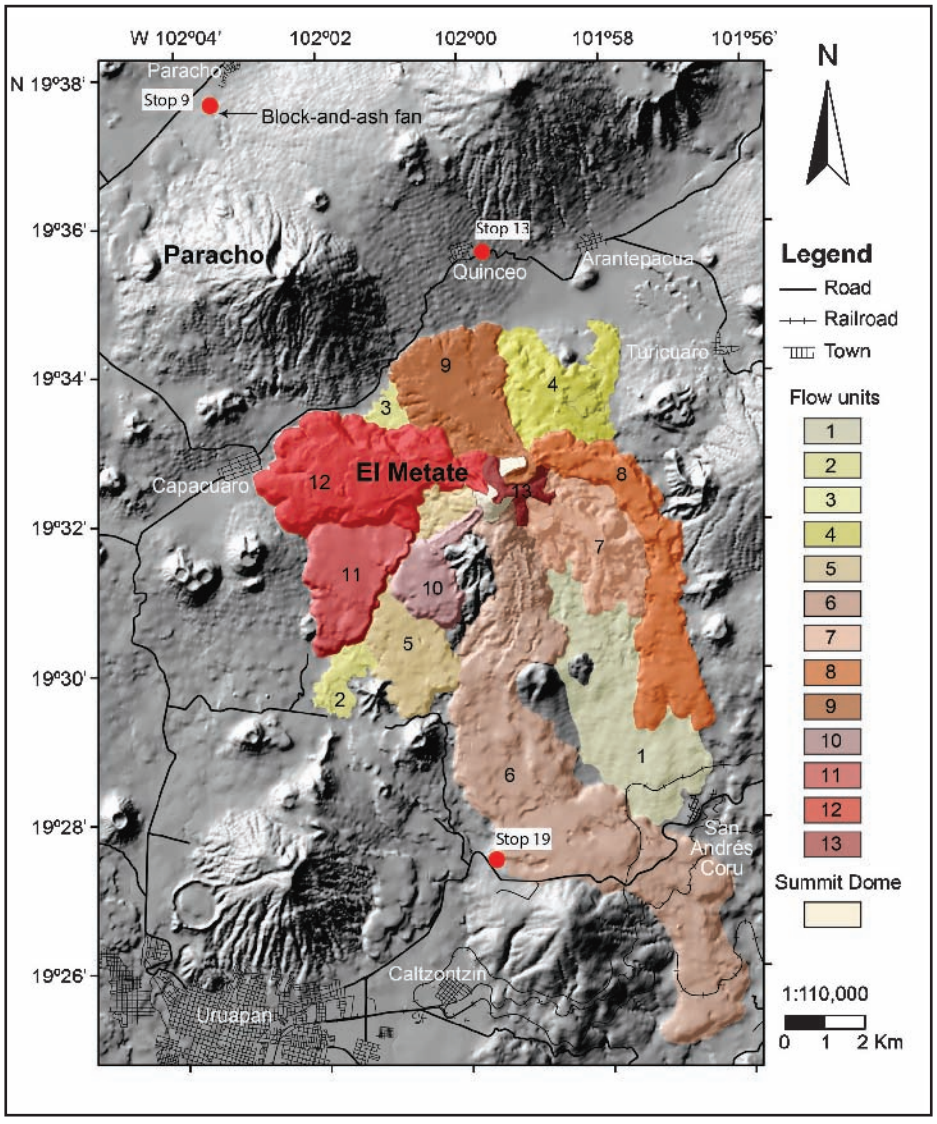

Figure 33: Hill-shade model showing the Cerro Paracho and Cerro El Metate area. The stratigraphic succession of El Metate lava flows (based on detailed mapping) is indicated. For location of this area see also Fig. 24.

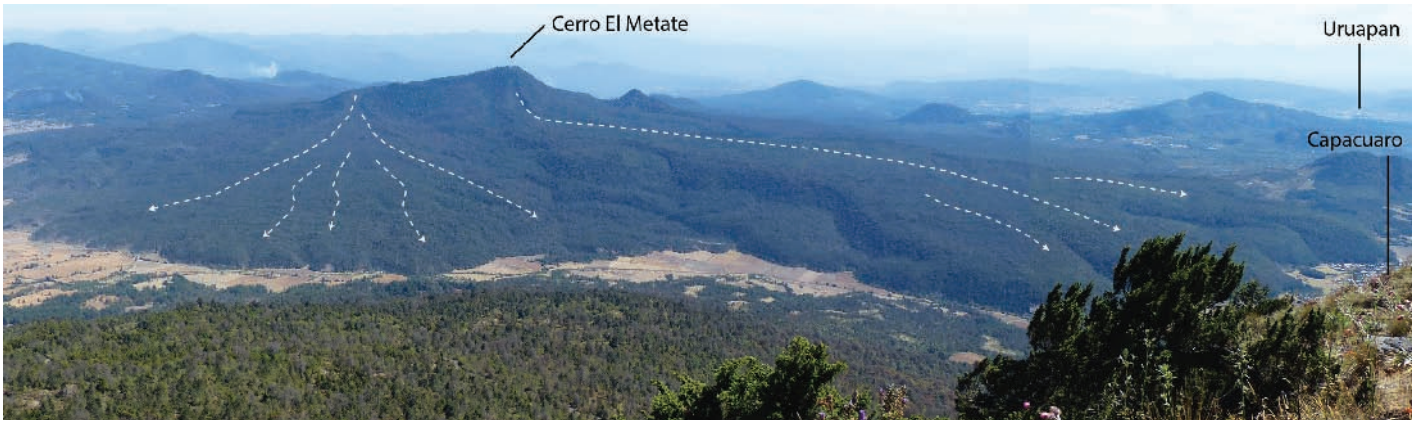

Figure 34: View of Cerro El Metate from Cerro Paracho. The dashed white arrows indicate the flow direction.

Figure 35: Raw "Metate" (rectangle-shaped, curved corn-grinding stone with a tripod) carved crudely at the quarry site on the upper slopes of El Metate volcano. Note flaking debitage on surrounding forrest ground. This first raw product is then transported by donkey from the quarry down-hill to the Purhépecha Indian town of Turícuaro. There it receives the finishing touches before being sold on local markets. We presume that this manufacture goes back to pre-Hispanic times and probably inspired the present Nahuatl name of this volcano.

entire volcano could have formed within 30 years. Such a short emplacement time is comparable to the duration of the nearby historical monogenetic Paricutin eruption (~10 years) but the erupted lava volume of El Metate is considerably larger (>11 km^3 vs. ~0.8 km^3 for Paricutin). This finding has substantial implications, especially for evaluating future hazards.

Furthermore, El Metate is also of interest for archaeological and ethnological reasons since specific parts of its lava flows near the summit (Fig. 33) are still being quarried today by local Purhépecha Indians to obtain the raw material needed for sculpting lithic tools including *metates* (flat corn-grinding stones with a rectangle shape, Fig. 35), *molcajetes* (mortars), and *manos* (pestles). Interestingly, most lava rocks do not meet the ideal requirements for these kitchen tools, which need to combine a certain porosity and texture of the material together with sufficient hardness. These kitchen tools have been used in the Mexican domestic environment since pre-Hispanic times.

DAYS 3 AND 4: EXCURSION TO PARICUTIN VOLCANO

During the next two days we will visit the principal sites of geological, cultural, and historical interest in the Paricutin area. The small picturesque town of Angahuan is the closest to the volcano (Fig. 36). It is located 23 km NW of the city of Uruapan, which announces itself as the "world capital of avocado". Uruapan can be reached from Morelia after a drive of 111 km (~1 hour) by taking the new toll road via Pátzcuaro. Hosting facilities are very limited in Angahuan (cabins at tourist center) but Uruapan offers multiple options for accommodation. The area is characterized by pine-and-oak forests and plantations of avocado trees. Temperatures at night can be relatively cold in the Paricutin area due to high altitudes (2400 masl at Angahuan, and 2770 masl at the summit of the Paricutin cone). Angahuan and other towns in the area are inhabited by Purhépecha (Tarascan) indians, many of which still speak their native language.

The Paricutin eruption – brief summary

The eruption of Paricutin started on February 20, 1943 and ended on March 4, 1952 (Wilcox, 1954). It produced ~0.64–0.7 km^3 of lava and 0.89–1.3 km^3 of tephra (Fries, 1953). The eruption was well documented (Luhr and Simkin, 1993). The onset of activity was preceded by 45 days of enhanced regional seismicity. The birth of the volcano was witnessed by at least four local people, including Dionisio Pulido, the owner of the cornfield where it occurred. The volcano first formed a <1 m-deep E-W-oriented fissure in alluvium that emitted ash, sulfur-rich gases, and incandescent bombs. A main cone grew rapidly, reaching 148 m in height at the end of the first month. Explosive activity was intense and often associated with lava effusion from separate vents. It was described as "violent Strombolian" (MacDonald, 1972; Pioli et

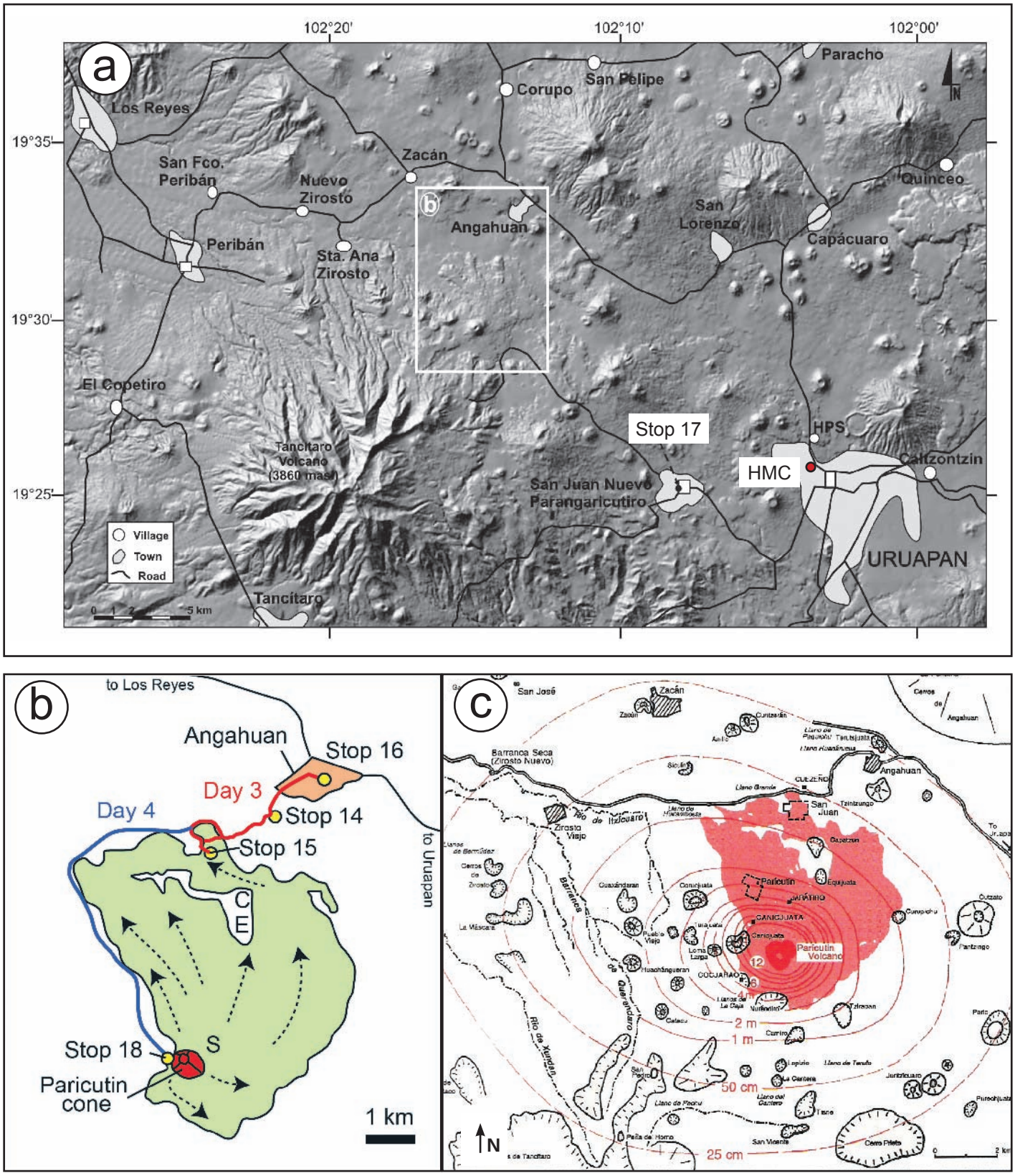

Figure 36: a) Digital elevation model of the Paricutin area indicating the main towns and villages and the hotel at Uruapan (Hotel Mansión Cupatitzio = HMC on map, other option is Hotel Pié de la Sierra = HPS on map). Note the large density of small volcanic cones in the area. b) Map of the itinerary of the excursion to the Paricutin area (Days 3 and 4) with Stops (Stop 17 is on a). Arrows denote flow directions. c) Map by Luhr and Simkin (1993) modified from Segerstrom (1950). Isopachs of ash fallout correspond to data collected on Oct. 1946 by K. Segerstrom. The location of the towns of Paricutin and San Juan Parangaricutiro destroyed by the lava flows is indicated, as well as the location of the town of Angahuan which was only affected by ash fallout and thus was not evacuated. The population of San Juan Parangaricutiro was relocated at San Juan Nuevo located 6 km W of Uruapan (Stop 17). People from Paricutin resettled at Caltzontzin, 5 km east of Uruapan (see Fig. 36a).

al., 2008). Eruptive clouds reached up to 8 km in height and fine ash fell on distant places, including Mexico City (350 km to the east) during the first days of April 1943. The intensity of the explosive activity and the volume of lava and tephra erupted, decreased gradually during the eruption as the magma flux declined (Fries, 1953). Products evolved in time from basaltic andesite to andesite (55–60 wt.% SiO_2), due to a combination of fractional crystallization and assimilation of the granitic basement (Wilcox, 1954; McBirney et al., 1987). The eruption had important social and economic impacts as two villages, San Juan Parangaricutiro (4000 inhabitants) and Paricutin (733 inhabitants), and a total of 24.8 km^2 of land were buried under lava (Luhr and Simkin, 1993). The vegetation was completely destroyed within an area of 300 km^2 covered by >15 cm of ash, which affected greatly the ecology and agriculture (Luhr and Simkin, 1993).

DAY 3: ANGAHUAN, PANORAMIC VIEW OF THE VOLCANO AND LAVA-FLOW FIELD, AND CHURCHES OF SAN JUAN PARANGARICUTIRO AND SAN JUAN NUEVO

This first day focuses on visiting villages affected by the eruption (town of Angahuan and church ruins of San Juan Parangaricutiro) and one of the sites where refugees were relocated permanently (San Juan Nuevo).

Itinerary: After a drive of 30 minutes (23 km) from Uruapan, Angahuan is reached (Figs. 36a, b). The town needs to be crossed in order to get to the tourist center (Stop 14). From a terrace in front of a cafeteria, a panoramic view of Paricutin and its lava flow-field can be enjoyed. From here, hike (ca. 40 minutes/ 2.5 km) or ride on horse to reach the edge of the Paricutin lava flows and the church ruins of Parangaricutiro (Stop 15). Return to Angahuan and visit its colonial church (Stop 16). After lunch, drive back to Uruapan (23 km) and from here to San Juan Nuevo (6 km) where the new church (Stop 17) is worth visiting.

Stop 14: Angahuan Tourist center "Las Cabañas" (19°32'26.5"; 102°14'3.8"; 2360 m)

This site provides a panoramic view of the Paricutin cone and the main part of

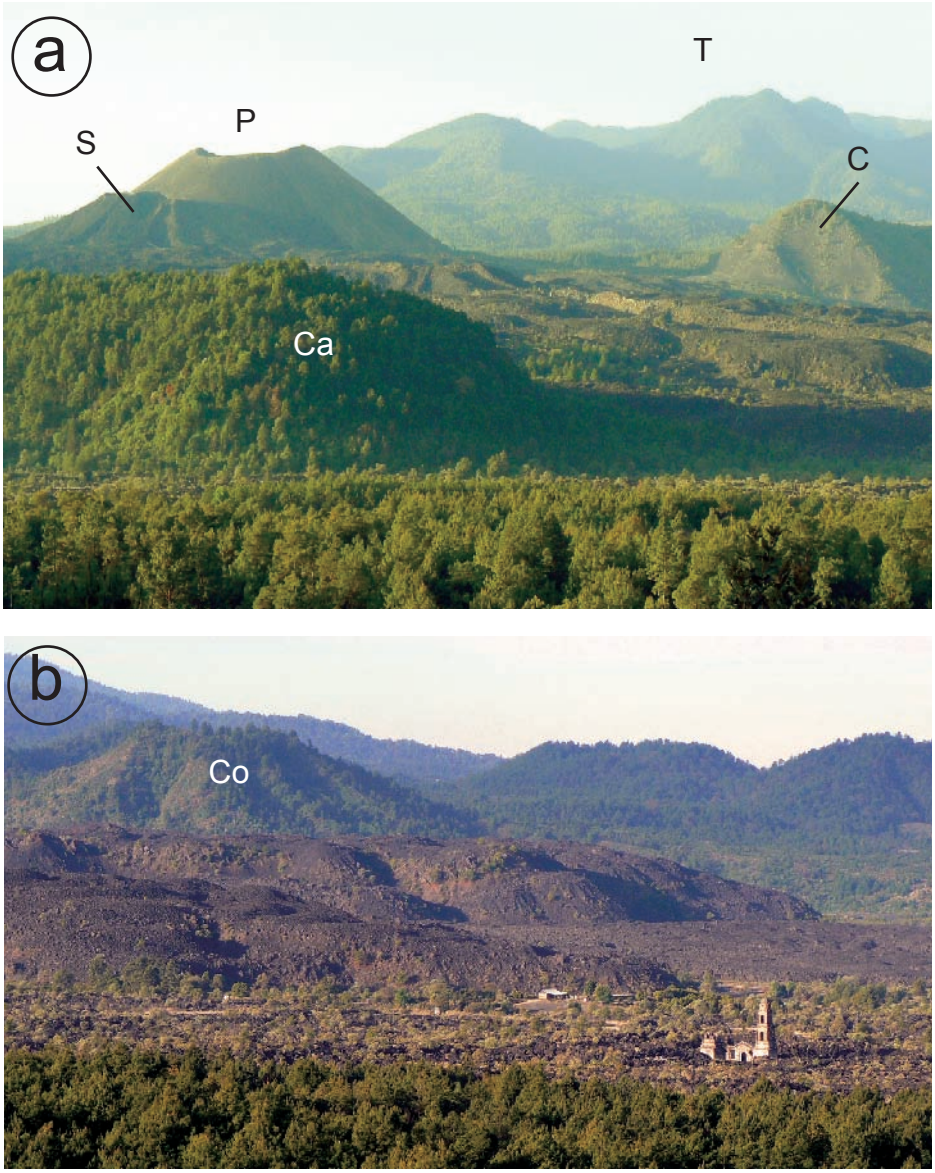

Figure 37: Panoramic views from terrace of Angahuan tourist center (Stop 14). a) View towards the south with Paricutin (P) and Sapichu (S) in front of Tancítaro (T). Older scoria cones Capatzun (Ca) and Canicjuata (C) are also indicated (see text for more details). b) View towards the SW showing the church ruins of San Juan Parangaricutiro engulfed by lava flows. Older scoria cone Corucjuata (Co) in background. Photos taken March 3, 2008.

Figure 38: Mural painting depicting the Paricutin eruption at the tourist center of Angahuan (see text for more details). Photo taken March 3, 2008.

the lava flow-field (Fig. 37). The northern flank of Paricutin, the NE parasitic Sapichu cone (observable also from the summit of Paricutin on Day 4), the church-ruin of San Juan Parangaricutiro partly buried by the lava (see Stop 15), and the older Capatzun (Ca in Fig. 37a) and Equijuata scoria cones surrounded by the flows can be observed from this location (Figs. 36b and 37). The Tancítaro stratovolcano (3840 masl) forms the elongated mountain in the background. When the sky is clear, especially at dusk or at dawn, it is also possible to see the Fuego and Nevado de Colima stratovolcanoes (located 125 km to the west) at the horizon.

Other points of interest in Angahuan (small visitor center) were constructed on the occasion of the 50th anniversary of the eruption in 1993. They include a colorful mural painting that can be seen along the walls of a cabin located along the path leading from the entrance to the panoramic viewpoint (Fig. 38). The painting features the Paricutin volcano at the center, and to the left, the destructive power of the eruption, as well as the suffering of the people whose dwellings were destroyed by the lava. To the right of the volcano, the return to harmony in the villages affected by the eruption is represented. A small museum exhibits photographs and contemporary news-clips reporting on the eruption.

Figure 39: Ruins of San Juan church (façade) invaded by lava flows on June 1944 (Stop 15). A copy in brick of the old church was built in San Juan Nuevo, where people from the old town resettled and the effigy of the "Lord of the Miracles" was transferred (Stop 17, Fig. 41). See text for more details. Photo taken March 3, 2008.

Stop 15: Visit of church ruins of San Juan Viejo Parangaricutiro (19°31'59.7"; 102°14'51.0"; 2280 m)

The volcano completely destroyed and buried two towns: Paricutin, located 2 km NNW of the eruption site and San Juan Parangaricutiro, ~4 km to the N (Fig. 36c). San Juan Parangaricutiro was the main populated center of this part of Michoacán before the eruption. About 4000 people lived in this small town originally named Parangaricutiro by the Purhépecha (Tarascan) and renamed San Juan by the Spaniards in 1530 (Foshag and González-Reyna, 1956). It was an important religious center and pilgrims would travel from the entire state of Michoacán to see the carved statue of the *Señor* or *Cristo de los Milagros* (Lord of the Miracles) displayed on the main altar within the church. The Paricutin volcano formed 4 km upslope from the small town, and a year and a half after the start of the eruption, the lava reached the outskirts of the town. On May 9, 1944, carrying the sacred statue and led by the local priest, the people left definitely the village and on May 11 they founded a new town, San Juan Nuevo (see Stop 17), 6 km west of Uruapan. By the end of July 1944, almost the entire village was buried under up to 15–20 m of lava. The tower and massive walls of the main building of the church are the only features that still protrude from the flows (Fig. 39). In contrast, nothing remains of the Paricutin village located closer to the volcano (Fig. 36b), which was invaded by the lavas on June 18, 1943, only 4 months after the start of the eruption. People from the Paricutin village resettled at Caltzontzin (Nolan, 1979), a village located at the outskirts of Uruapan (Figs. 24 and 36a).

Today, a path cuts across the flows and leads to the remains of the church (Fig. 39). Note that the surface of the lava flows is composed of torn and twisted clinkery blocks. These flows were emplaced as distinct viscous lobes breaking out from a rapidly advancing flow front, which contrasts with most lavas produced during the eruption that advanced as A'a flows (Foshag and González-Reyna, 1956). The distal flow front at this location is situated only 120 m from the church, almost 4 km from the vent.

Stop 16: Visit of Angahuan church (19°32'50.7"; 102°13'27.9"; 2390 m)

Angahuan is a traditional Purhépecha village characterized by wooden houses. Older local people, women, and young girls are dressed in traditional colorful costumes and many still speak the Purhépecha language. Marks of modernity have however reached this relatively remote and conservative part of Mexico and houses built with cement are increasingly common, as well as locals wearing "normal" clothes (men in particular).

The eruption of Paricutin greatly impacted the lives of the Angahuan people (Rees, 1979; Nolan, 1979). Traditional activities such as agriculture and cattle raising were rendered impossible due to the thick ash fallout, and the development of tourism provided a vital new source of income for the local people. Today, tourist guiding, horse rental, and handcrafting represent important revenue for the expanding population.

The church of Angahuan at the main central square (Fig. 40) was built around 1560 by Franciscan friars. Completely ignored prior to the eruption, it has since gained considerable interest from art historians. The elaborate doors of the church contrast greatly with the austere building. They contain elements of arab, gothic, and renaissance style (Rodríguez-Elizarrarás et al., 1993, and references therein for additional information).

A wooden door of a private house

Figure 40: Angahuan colonial church (Stop 16). a) Main entrance to the church. Photo taken August 15, 2009. b) Close-up of the image of Saint Jacob carved in stone (fine-grained ignimbrite) above the main entrance. Photo taken March 2, 2008.

within the village used to display carvings that pictured the main stages of evolution of the volcano (Fig. 10 in Rodríguez-Elizarrarás et al., 1993). Unfortunately, this door does not exist anymore but a reproduction can be found at the entrance of a souvenir store located on the main street leading to the visitor center.

Stop 17: Church of San Juan Nuevo (19°24'58.9"; 102°07'44.3"; 1870 m)

This small town was founded on May 10, 1944 by the people of the original town of San Juan Parangaricutiro (San Juan Viejo) invaded by the Paricutin lava flows. The modern church (Fig. 41a) visited by thousands of pilgrims each year is the main attraction of the town. It is a copy in brick of the ancient stone church partly buried by the lava (Stop 15). Large colorful paintings displayed inside the church relate the history of the town including the fatal destruction by the lavas, the exodus, and relocation of the people at the new site (Fig. 41b). The original sacred effigy of the *Señor de los Milagros* is displayed on the main altar of the church.

An organization of the indigenous community of San Juan recently received an award from the United Nations (Equator Price 2004; http://www.equatorinitiative.org). This distinction rewards the efforts of the community for developing a sustainable exploitation of the local forest resources that contributes to the economy of the town.

DAY 4: HORSE-RIDE TO THE PARICUTIN CONE (STOP 18)

The objective of this day is to climb to the summit of the Paricutin cone starting at the visitor center of Angahuan. Horses are the easiest and most rapid means to get to the base of the cone. The path used (~11 km/ 4 hours from Angahuan to the summit) avoids the N and NW lava flows (see Fig. 36b). For additional Stops that can be made see Rodríguez-Elizarrarás et al. (1993).

After a horse-ride of ~3 hours (don't forget your *sombrero*), the W base of the cone is reached. After dismounting and securing the horses under the shade of a group of pine trees, the cone can be climbed in 45 to 60 minutes, following a path that goes diagonally to the S crater rim and circumnavigates the crater. The climb is somewhat tedious, because of the fragmented nature (scoria and ash) of the loose material forming the slopes. The descent is much faster and starts from the main summit on the W crater rim and goes straight down to the groove of trees where the horses were left behind. Consider that on the crater rim the wind is often strong (watch your *sombrero*) and temperatures are fresh (bring your jacket) as the summit culminates at ~2800 masl. The cone is 220 m high and 950 m wide at the base. The crater has a diameter of 250 m and a depth of ~40 m.

The evolution of the cone during the eruption is well documented (see Luhr and Simkin, 1993, Fig. 42). It grew mostly during the first year. By the end of the first day it was already 30 m high (nearly 1 m/ hr), doubled in height by the end of the third day, and reached 148 m in height at the end of the first month (average of 5 m/day). By the end of the first year it was 336 m high (almost 1 m/day on average). In the following 8 years it grew slowly, finally reaching its maximum height of 424 m in 1952. Note that lava flows covered the base so that the height of the cone protruding from the flows is lower (220 m) than its actual height (424 m, see above). The cone growth was not continuous. Eyewitnesses describe several

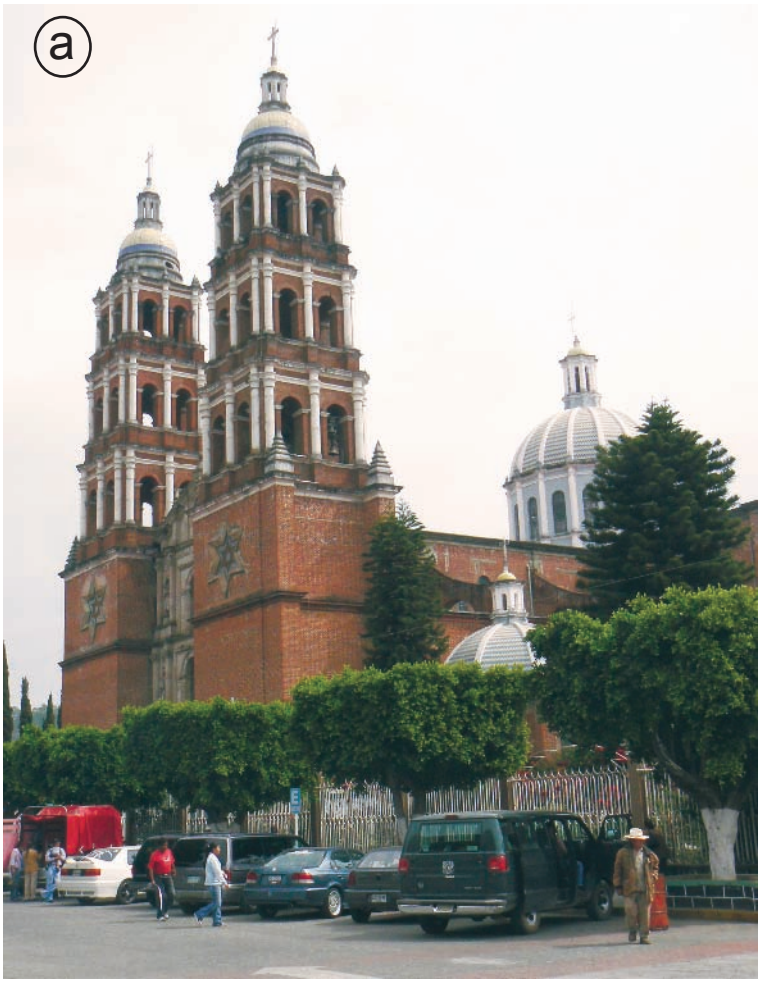

Figure 41: a) Modern church of San Juan Nuevo (Stop 17). This church is the meeting place of thousands of pilgrims who travel each year to San Juan Nuevo in order to pray to the Lord of the Miracles exposed on the main altar. This effigy was rescued from the old church just prior to its inundation by the lava flows. b) Detail of painting in the interior of the church describing the disaster and exodus of the people from San Juan Parangaricutiro. Photos taken March 4, 2008.

episodes of partial destruction (e.g. Ordóñez, 1947; Foshag and González-Reyna, 1956). Flank collapses were accompanied by lateral lava outbreaks. At the beginning of the eruption, lava emerged from vents formed within the cone and flowed out from the opening in the cone left by the collapse. Later in the eruption, when the cone had reached maturity, lava was emitted from temporary vents formed at the base of the cone. During pauses in lava emission, explosive activity at the cone rapidly healed the breaches, restoring the cone's symmetry (Luhr and Simkin, 1993; Foshag and González-Reyna, 1956; see also painting by Dr. Atl on back cover). It is remarkable that the current shape of the cone does not record any of these episodes of destruction and reconstruction (Fig. 43, see also photo on back cover).

The path along the crater rim (Fig. 43b) provides an overview of the lava flow-field and the surrounding area. The high density of young scoria cones in the region surrounding the Paricutin is spectacular. From the rim, it is possible to distinguish several different lava branches that piled up with time. As during the Jorullo eruption (Guilbaud et al., 2009) the flows that reached the furthest distance from the vent were the earliest produced (Fig. 44), because of the increase in the magma's silica content and thus viscosity with time. However, the lava flow-field is much more complex than at Jorullo and despite the careful monitoring of the eruption, an exact map of the different flow units could not be constructed (Luhr and Simkin, 1993).

From the NE rim looking north, notice the Sapichu vent (from *Zapicho*, Tarascan word for kid or small boy, Ordóñez, 1947) (Fig. 43). This vent, built 8 months after the beginning of the eruption, emitted lava continuously during its 2.5 months of activity. It thus never formed a complete cone but an irregular-shaped edifice. Fumarole gases still escape from its summit and form whitish coatings (Fig. 43b). Other hot fumarolic areas in the dark-colored flow-field can be seen from the crater rim, distinguishable by their contrasting whitish coloration. A 270°C fumarole sampled in June 1995 contained 47 mol-% CO_2 and 52 mol-% air (water free basis). The carbon-13 isotope value of –20.5 ‰ for the CO_2 indicates that the hot interior of the flow was still thermally decomposing organic debris near the flow base 50 years after eruption (Goff and McMurtry, 2000).

DAY 5: EL METATE LAVA FLOW AND DRIVE TO QUERÉTARO VIA PÁTZCUARO (EARLY COLONIAL CAPITAL OF MICHOACÁN) AND CUITZEO (16TH CENTURY MONASTERY)

On this day, a large quarry that exposes the interior of the southern El Metate lava flow not far from Uruapan will be visited (Stop 19). Then, we will have a coffee-break at the main square of Pátzcuaro (Stop 20), surrounded by colonial buildings. From there we will head towards Cuitzeo, where we will visit a 16th century monastery (Stop 21) and have lunch, before driving to Querétaro. The trip will end at the conference venue near Juriquilla.

Itinerary: Exit Uruapan and head northeast on old (toll-free) federal highway No. 14. After 2.5 km and a narrow curve to the right, the road becomes steeper (starts climbing up the lateral margin of El Metate lava flow). After a few hundred meters, turn left and enter large quarry operation (Stop 19, Figs. 24, 25, 33). After inspecting the exposure of the internal features of El Metate lava flow (Fig. 45), return to the paved highway (Fig. 2), continue east, cross Tingambato, and arrive at Pátzcuaro (60 km/75 Mins.). After enjoying a stroll and coffee-break at the main square (Stop 20) continue northeast to Morelia on highway No. 14 (Fig. 2). Avoid entering the center of Morelia and take "Periférico" that surrounds the city on its western margin. Exit Morelia to the North on highway No. 43 (in direction to Salamanca), cross toll-road Guadalajara-Mexico-City, traverse the lacustrine plain of Cuitzeo lake and arrive at the main square (Stop 21) of the town of Cuitzeo (92 km/100 Mins for the entire stretch from Pátzcuaro to Cuitzeo). After visiting the 16th century monastery and having lunch at the main square, continue north on toll-road No. 43 until Salamanca (Fig. 1). From here continue east on toll-road No. 45 toward Querétaro and Hotel Juriquilla, the 5IMC conference venue (190 km/ 160 Mins.)

Stop 19: Quarry at southern El Metate lava flow (19°27'38.8"; 101°59'34.9"; 1868 m)

This large quarry has been excavated into the lateral margin of the longest lava flow that issued from El Metate (Flow 6 in Fig.

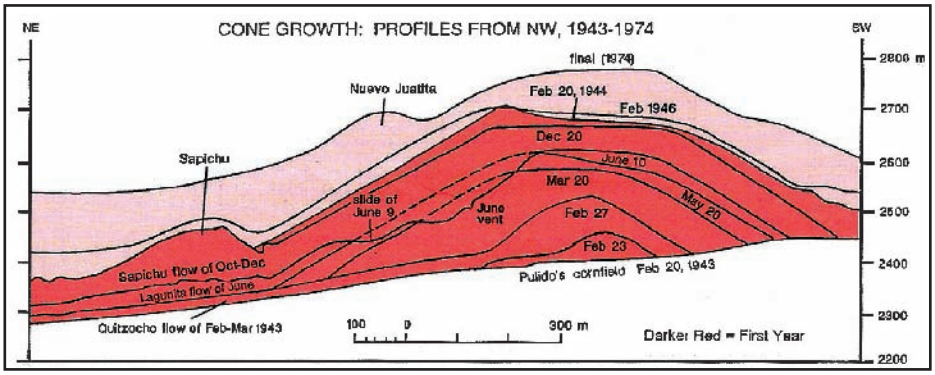

Figure 42: Sketch of the main stages of the construction of the Paricutin cone (from Luhr and Simkin, 1993). Note that the cone was mainly built during the first year of the eruption.

Figure 43: a) View of the Paricutin cone from the path surrounding the western margin of the flow-field. Horses are dismounted at the foot of the cone (white arrow). Photo taken March 3, 2008. b) Aerial view of the crater towards the north showing formation of gullies (arrow 1) and enigmatic concentric (wind-blown?) features (arrow 2). Fumaroles at Sapichu (S) and point of descent (D) back to horses are also indicated. Photo taken January 31, 2009.

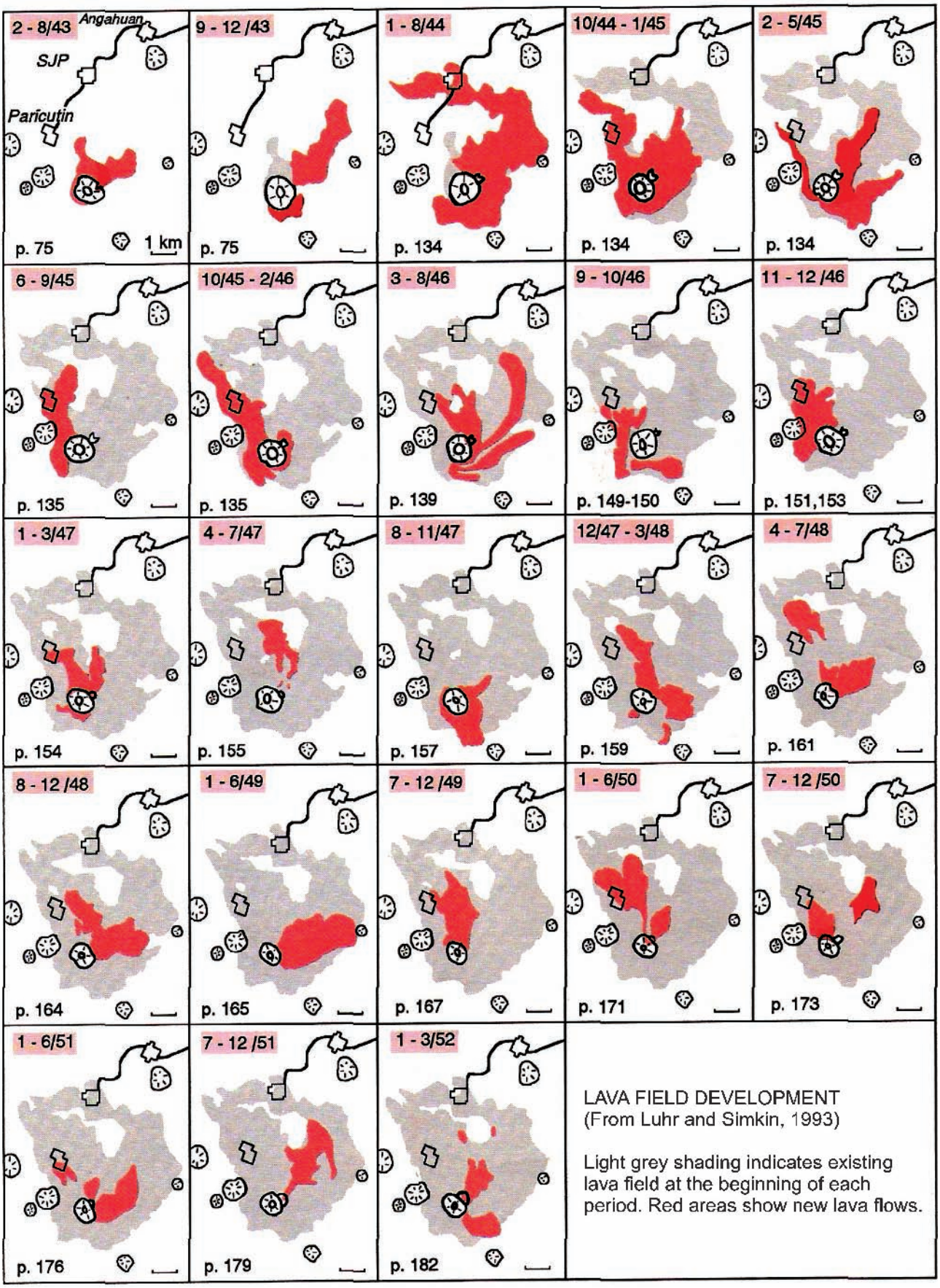

Figure 44: Map showing the chronological sequence in which the Paricutin lavas were emplaced (from Luhr and Simkin, 1993).

33). This flow is about 15 km long, 2.5 km wide, may have a thickness of up to 80 m, and a volume of ~3.4 km^3. The flow has a blocky (fractured) surface covered by several meters of debris. A simple concept that helps envisage the mode of emplacement of such a flow is the "caterpillar advance" model. Accordingly, only the dense fluid core of the flow does actually flow carrying blocky rigid fragments of its broken carapace on top. Blocks fall off the flow front and are buried underneath as the flow advances, generating at the bottom a breccia layer and levées (elongate piles of debris) at its lateral margins. The morphology of this flow resembles that of glaciers, which are also slowly moving sheets of material that flow at their base and have a fractured surface covered by accumulated debris, forming lateral and frontal moraines (similar to lava flow levées).

This outcrop (Fig. 45) displays the interior structure of the levée of the lava flow. At first sight, the upper part of the exposure (Fig. 45a) resembles that of a pyroclastic block-and-ash flow (angular blocks embedded in a sandy matrix). The blocky upper part of the flow displays a highly autobrecciated structure in its interior that resulted from friction and associated shear stresses caused by the force of the advancing lava flow. In the lower part of the outcrop (Fig. 45b), the dense core of the flow is fractured but still intact. It overlies another breccia layer that is 50 m above the base of the flow. The fractured core and brecciated layer provide evidence for the complex mode of emplacement of such high-viscosity flows.

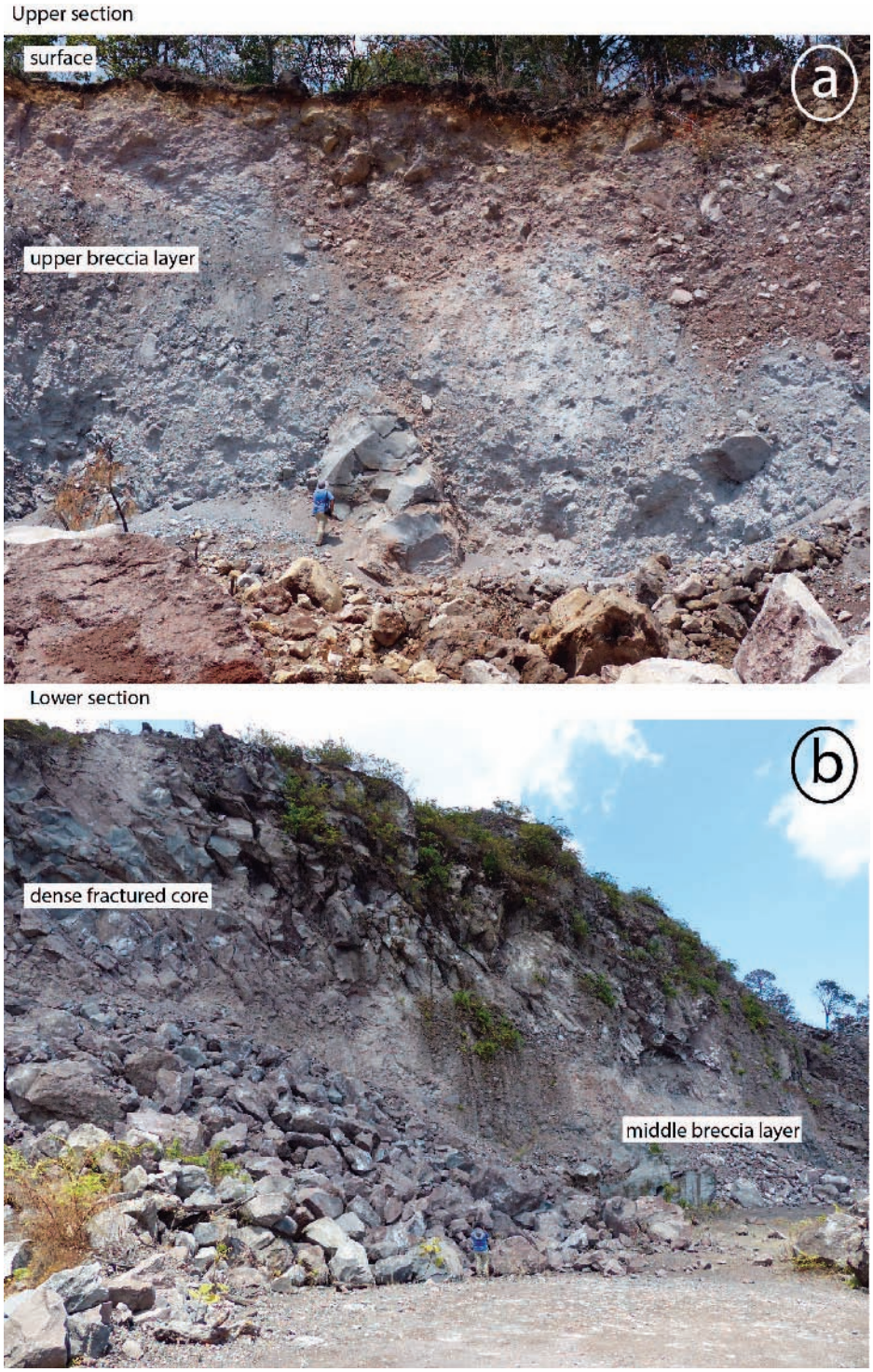

Figure 45: Quarry at El Metate lava flow levée (Stop 19). a) Uppermost section of the levée displaying 10 m thick autobrecciated layer containing blocks (several m in size) embeded in a sandy-gravelly matrix. b) Few meters below a) this lower part of the outcrop shows the dense fractured core of the lava flow resting on yet another thick breccia layer.

Stop 20: Pátzcuaro (19°30'48.5"; 101°36'33.0"; 2160 m)

Pátzcuaro, located on the southern shore of the lake with the same name (Fig. 2), is certainly one of the most charming cities of Mexico. Its colonial architecture (especially edifices built during the 18th century) includes religious buildings (churches and monasteries) as well as luxurious civil mansions with beautiful interior patios of extraordinary artistic value. In addition, traditional markets, museums, and surrounding picturesque villages are worth visiting and could easily fill an itinerary of several days. The main square (Plaza Vasco de Quiroga) with its surrounding arches (Fig. 46) is an ideal starting point for a reconnaissance tour of the central part of town.

Pátzcuaro was the first capital of the Tarascan kingdom before it was moved to Tzintzuntzan, also located at the lake, but further to the north (Fig. 2). Its temperate climate was considered healthy (mean annual Temp. = 16.4 °C). In 1534, shortly after the Spanish conquest, Vasco de Quiroga was appointed the first bishop of the province of Michoacán, which was initially seated at Tzintzuntzan, the center of the former Tarascan kingdom and most densely populated area in the region. He decided to move the seat of the bishopric from Tzintzuntzan to nearby Pátzcuaro in 1538 and there he constructed the first cathedral on top of the old Tarascan temples (Warren, 1985). A few decades later, the silver mines of Guanajuato to the north

Figure 46: Main square of Pátzcuaro surrounded by arcades and colonial buildings (Stop 20).

Figure 47: Augustinian monastery at Cuitzeo, erected during the 16th century in early colonial time (Stop 21).

(Fig. 1) were discovered. Since Pátzcuaro was somewhat off from the main road between the cities of Mexico and Guanajuato, Valladolid (now Morelia) located closer, started to gain in importance as a center of food supplies, etc. for the new mining operations in the northern part of New Spain. As a result, the seat of the bishopric was moved to Valladolid (Morelia) in 1574 and Pátzcuaro lost the cathedral. In addition, during epidemic diseases of 1576-1578, Pátzcuaro lost a substantial percentage of its Indian population. Nonetheless, due to its strategic geographic position at the southern margin of the Mexican high plateau and gate to the *Tierra Caliente* to the south, Pátzcuaro recovered and benefited from trading with this vast area that included the port of Acapulco, which received goods from China (e.g. textiles, porcelain, spices) and Perú (quicksilver). Although the *Tierra Caliente* was considered unhealthy and was, hence, sparsely populated, it did produce important commodities such as sugar, cotton, copper, etc. that were in high demand in the highlands. The economic bonanza in the silver-mining districts of Guanajuato and Zacatecas also had repercussions in Pátzcuaro, which experienced a construction boom between 1740 and 1760. Most of the baroque private mansions at the main square were built during this period and many religious and public buildings refurbished.

Stop 21: Cuitzeo (19°58'08.4"; 101°08'22.9"; 1852 m)

The Augustinian monastery of Santa María Magdalena in Cuitzeo (Fig. 47) is one of the most sumptuous 16th century buildings of Michoacán. Its construction goes back to the 1550s when Augustinian monks had the ancient pre-Hispanic temple at the shore of the lake demolished and used the cut stone from the old building for the foundations of the new church. The sculpted church facade is of particular interest and artistic quality. Christian symbolism (e.g. the pierced heart of St. Augustine) and Spanish royal emblems (e.g. the Hapsburg two-headed eagle) are artfully integrated with native motives into the facade. Also of interest is the adjacent convent, the elaborately framed open chapel and a 16th century fresco depicting the Last Judgement.

ACKNOWLEDGEMENTS

Fraser Goff (Los Alamos, New Mexico) made suggestions for improving a first draft of the manuscript. Field and laboratory costs were defrayed from projects funded by the Consejo Nacional de Ciencia y Tecnología (CONACyT-167231 and 152294) and the Dirección General de Asuntos del Personal Académico (UNAM-DGAPA IN-109412-3 and IB102312) granted to Claus Siebe and Marie-Noëlle Guilbaud. Pooja Kshirsagar and Oryaëlle Chevrel were funded by UNAM-DGAPA postdoctoral fellowships. Juan Ramón de la Fuente and Athziri Hernández Jiménez received graduate stipends from CONACYT.

REFERENCES

Aranda-Gómez, J.J., Levresse, G., Martínez, J.P., Ramos-Leal, J.A., Carrasco-Núñez, G., Chacón-Baca, E., González-Naranjo, G., Chávez-Cabello, G., Vega-González, M., Origel, G., Noyola-Medrano, C., 2013. Active sinking at the bottom of the Rincón de Parangueo Maar (Guanajuato, México) and its probable relation with subsidence faults at Salamanca and Celaya. Boletín de la Sociedad Geológica Mexicana 65 (1): 169-188.

Arnauld, C., Carot, P., Fauvet-Berthelot, M.-F., 1994. Introducción. In: Pétrequin, P. (Ed.): 8000 años de la Cuenca de Zacapu. Evolución de los paisajes y primeros desmontes. Collection Etudes Méso-américaines II-14: 9-28, CEMCA, México, D.F.

Artigas, J.B., 2001. Pueblos-hospitales y guatáperas de Michoacán. Las realizaciones arquitectónicas de Vasco de Quiroga y fray Juan de San Miguel. UNAM-Gobierno del Estado de Michoacán, 141 pp.

Artigas, J.B., 2010. Mexico-Arquitectura del siglo XVI. Santillana Ediciones, México, D.F., 608 pp.

Ban, M., Hasenaka, T., Delgado-Granados, H., Takaoka, N., 1992. K-Ar ages of lavas from shield volcanoes in the Michoacán-Guanajuato volcanic field, México. Geofis. Int. 31 (4): 467-473.

Connor, C. B., 1987. Structure of the Michoacán-Guanajuato Volcanic Field, Mexico. J. Volcanol. Geotherm. Res. 33: 191-200.

Correa-Metrio, A., Lozano-García, S., Xelhuantzi-López, S., Sosa-Nájera, S., Metcalfe, S. E., 2012. Vegetation in western Mexico during the last 50,000 years: modern analogs and climate in the Zacapu basin. J. Quat. Sci. 27 (5): 509-518.

Demant, A., 1992. Marco geológico regional de la laguna de Zacapu, Michoacán, México. In: Demant, D., Labat, J.-N., Michelet, D., Tricart, J., (Eds.), El Proyecto Michoacán 1983-1987. Medio ambiente e introducción a los trabajos arqueológicos. Collection Etudes Mésoaméricaines II-11: 53-72, CEMCA, México, D.F.

Foshag, W.F., González-Reyna, J.R., 1956. Birth and development of Paricutin Volcano Mexico: U.S. Geol. Survey Bull. 965D: 355–489.

Fries, C.Jr., 1953. Volumes and weights of pyroclastic material, lava, and water erupted by Parícutin Volcano, Michoacán, Mexico: Trans. Am. Geophys. Union (EOS) 34: 603–616.

Goff, F., McMurtry, G.M., 2000. Tritium and stable isotopes of magmatic waters. J. Volcanol. Geotherm. Res. 97:347-396.

Guilbaud, M.N., Siebe, C., Salinas, S., 2009. Excursions to Paricutin and Jorullo (Michoacán), the youngest volcanoes of the Trans-Mexican Volcanic Belt. A commemorative fieldtrip on the occasion of the 250th anniversary of Volcán Jorullo's birthday on September 29, 1759. Impretei S.A., México, D.F., 31 p.

Guilbaud, M-N., Siebe, C., Layer, P., Salinas, S., Castro-Govea, R., Garduño-Monroy, V.H., Le Corvec, N., 2011. Geology, geochronology, and tectonic setting of the Jorullo Volcano region, Michoacán, México. J. Volcanol. Geotherm. Res. 201: 97-112.

Guilbaud, M-N., Siebe, C., Layer, P., Salinas, S., 2012. Reconstruction of the volcanic history of the Tacámbaro-Pururarán area (Michoacán, México) reveals high frequency of Holocene monogenetic eruptions. Bull. Volcanol. 74: 1187-1211.

Hasenaka, T., Carmichael, I.S.E., 1985. The cinder cones of Michoacán-Guanajuato, Central Mexico: Their age, volume and distribution, and magma discharge rate. J. Volcanol. Geotherm. Res. 25: 105-124.

Hasenaka, T., Carmichael, I.S.E., 1986. Metate and other shield volcanoes of the Michoacan-Guanajuato, Mexico. Trans. Am. Geophys. Union (EOS) 67: 44.

Hasenaka, T., Carmichael, I.S.E., 1987. The cinder cones of Michoacán-Guanajuato, Central México: Petrology and chemistry. J. Petrol. 28: 241-269.

Hasenaka, T., 1994a. Size, distribution and magma output rates for shield volcanoes of the Michoacán-Guanajuato volcanic field, Central Mexico. J. Volcanol. Geotherm. Res. 63:13– 31.

Hasenaka, T., Ban M., Delgado-Granados, H., 1994b. Contrasting volcanism in the Michoacán-Guanajuato volcanic field, Central Mexico: Shield volcanoes vs. cinder cones. Geof. Int. 33 (1): 125-138.

Kshirsagar, P., Siebe, C., Guilbaud, M.-N., Salinas, S., 2014. Hydrogeological setting and stratigraphy of the Alberca de Guadalupe maar volcano at the SE margin of the Zacapu basin, Michoacán, México. IAVCEI-5IMC-Conference, Querétaro, Mexico.

Luhr, J.F., Simkin, T., 1993. Parícutin: The volcano born in a Mexican cornfield. Geoscience Press, Phoenix, Arizona, 427 pp.

Lumholtz, C., Hrdlicka, A., 1898. Marked human bones from a Prehistoric Tarasco Indian burial place in the State of Michoacan, Mexico. Bull. Am. Museum Nat. Hist. X: 61-79 (Plates V-IX). New York.

MacDonald, G.A., 1972. Volcanoes: New Jersey, Englewood Cliffs, Prentice Hall Inc., 510 pp.

Maciel-Peña, R., Goguitchaichvili, A., Guilbaud, M.N., Ruiz-Martínez, V.C., Calvo-Rathert, M., Siebe, C., Aguilar-Reyes, B., Morales, J., 2014. Paleomagnetic secular variation study of Ar-Ar dated lava flows from Tacámbaro area (Central Mexico): Possible evidence of Intra-Jaramillo geomagnetic excursion in volcanic rocks. Phys. Earth Planet. Int. 229: 98-109.

McBirney, A.R., Taylor, H.P., Armstrong, R.L., 1987. Paricutin re-examined: a classic example of crustal assimilation in calc-alkaline magma. Contr. Mineral. Petrol. 95: 4-20.

Metcalfe, S.E., 1992. Changing environments of the Zacapu Basin, Central Mexico: A diatom-based history spanning the last 30,000 years. Research Paper N. 48, School of Geography, University of Oxford.

Metcalfe, S.E., 1995. Holocene environmental change in the Zacapu Basin, Mexico: a diatom based record. Holocene 5: 196-208.

Metcalfe, S.E., Harrison, S.P., 1984. Cambio ambiental del Cuaternario Tardío en depósitos lacustres en la cuenca de Zacapu, Michoacán. Reconstrucción preliminar. Boletín del Instituto de Geografía 14: 127-151, UNAM, México.

Newton, A.J., Metcalfe, S.E., Davies, S.J., Cook, G., Barker, P., Telford, R.J., 2005. Late Quaternary volcanic record from lakes of Michoacán, central México. Quat. Sci. Rev. 24: 91-104.

Nolan, M.L., 1979. Impact of Paricutin on five communities. In: Sheets, P.D., and Grayson, D.K. (Eds): Volcanic activity and human ecology. New York, Academic Press, p. 293–338.

Noriega E., Noriega, A., 1923. La desecación de la ciénega de Zacapu y las leyes agrarias. Caso especial, único en el país. México.

Ordóñez, E., 1947. El volcán de Paricutin: México, Editorial Fantasía, 181 p.

Ortega, B., Caballero, C., Lozano, S., Israde, I., Vilaclara, G., 2002. 52 000 years of environmental history in Zacapu basin, Michoacán, México: the magnetic record. Earth Planet. Sci. Lett. 202: 663-675.

Ownby, S., Delgado-Granados, H., Lange, R.A., Hall, C.M., 2006. Volcán Tancítaro, Michoacán, México. 40Ar/39Ar constraints on its history of sector collapse. J. Volcanol. Geotherm. Res. 161: 1-14.

Ownby, S.E., Lange, R. A., Hall, C.M., Delgado-Granados, H., 2011. Origin of andesite in the deep crust and eruption rates in the Tancítaro-Nueva Italia region of the central Mexican arc. Bull. Geol. Soc. Am. 123 (1-2): 274-294.

Pereira, G., 2005. The utilization of grooved human bones: A reanalysis of artificially modifified human bones excavated by Carl Lumholtz at Zacapu, Michoacán, Mexico. Latin Am. Antiquity 16 (3): 293-312.

Perry, R.D., 1997. Blue lakes and silver cities. The colonial arts and architecture of West Mexico. Espadaña Press, 272 p.

Pétrequin, P., 1994. 8000 años de la cuenca de Zacapu, Céntre de Etudes Mexicaines et Centroamericaines, Mexico. Cuadernos de Estudios Michoacanos 6, 144 p.

Pioli, L., Erlund, E., Johnson, E.R., Cashman, K.V., Wallace, P.J., Rosi, M., Delgado, H., 2008. Explosive dynamics of violent Strombolian eruptions: The eruption of Paricutin Volcano 1943–1952 (Mexico): Earth Planet. Sci. Lett. 271: 359–368.

Rees, J.D., 1979. Effects of the eruption of Paricutin volcano on landforms, vegetation, and human occupancy. In: Sheets, P.D., and Grayson, D.K. (Eds.): Volcanic activity and human ecology: New York, Academic Press, p. 249–292.

Reyes-García, C., Gougeon, O., 1991. Paisajes rurales en el norte de Michoacán. Cuadernos de Estudios Michoacanos No. 3, El Colegio de Michoacán-Centre D'Etudes Mexicaines et Centraméricains, Mexico, 104 p.

Rodríguez-Elizarrarás, S., Komorowski, J-C., Jiménez, V., Siebe, C., 1993. Guidebook for a geological excursion to Paricutin volcano, State of Michoacán, México: Mexico, Codex Editores, Universidad Nacional Autónoma de México, Instituto de Geología, 47 p.

Roggensack, K., 1992. Petrology and geochemistry of shield volcanoes in the central Mexican Volcanic Belt. PhD-thesis, Dartmouth College, Hanover, New Hampshire, 179 p.

Segerstrom, K., 1950. Erosion studies at Paricutin, State of Michoacán, Mexico: U.S. Geol. Survey Bull. 965A: 1-164.

Siebe, C., Guilbaud, M.N., Salinas, S., Chedeville-Monzo, C. 2012. Eruption of Alberca de los Espinos tuff cone causes transgression of Zacapu lake ca. 25,000 yr BP in Michoacán, Mexico. 4IMC Conference, Auckland, NZ. Abstract volume. Geoscience Society of New Zealand Miscellaneous Publication 131A: 74-75.

Siebe, C., Guilbaud, M-N., Salinas, S., Layer, P.W., 2013. Comparision of the volcanic geology of the Tacámbaro-Puruarán (arc front) and the Zacapu (arc inland) areas in the Michoacán-Guanajuato volcanic field, Mexico. IAVCEI 2013 Scientific Assembly, July 20-24. Kagoshima, Japan, Abstract Volume.

Siebe, C., Salinas, S., 2014. Distribution of monogenetic phreato-magmatic volcanoes (maars, tuff-cones, tuff-rings) in the Mexican Volcanic Belt and their tectonic and hydrogeologic environment. IAVCEI-5IMC-Conference, Querétaro, Mexico.

Telford, R., Barker, P., Metcalfe, S., Newton, A. 2004. Lacustrine responses to tephra deposition: Examples from Mexico. Quat. Sci. Rev. 23: 2337-2353.

Tricart, J., 1992. La cuenca lacustre de Zacapu: Un acercamiento geomorfológico. In: Demant, D., Labat, J.-N., Michelet, D., Tricart, J., (Eds.), El Proyecto Michoacán 1983-1987. Medio ambiente e introducción a los trabajos arqueológicos. Collection Etudes Mésoaméricaines II-11: 113-197, CEMCA, México, D.F.

Warren, J.B., 1985. The conquest of Michoacán. Norman, Oklahoma University Press, 352 p.

Whitford-Stark, J.L., 1975. Shield Volcanoes. In: G. Fielder and L. Wilson (Eds.): Volcanoes of the Earth, Moon and Mars, St. Martins Press, New York, NY, pp. 66-74.

Wilcox, R.E., 1954. Petrology of Paricutin Volcano, Mexico: U.S. Geol. Survey Bull. 965C: 281–349.

Williams, H., 1950. Volcanoes of the Paricutin region, México: Geologic investigations in the Paricutin area, México. US Geol. Survey Bull. 965-B: 165-279.

Monogenetic volcanism of the Michoacán-Guanajuato volcanic field, México: Maar craters of the Zacapu basin and scoria cones of the Paricutin region

Se terminó de imprimir en noviembre del 2014, en los talleres de Impretei, S.A. de C.V.
Almería No. 17, Col. Postal, 03410
México, D.F. Tel. 5696-2503
impreteisa@prodigy.net.mx

El tiraje consta de 500 ejemplares
más sobrantes para su reposición

Front-cover:
Aerial photo of Alberca de Guadalupe maar crater from the east. Note normal fault displacing cliff-forming lava in the interior crater wall. Photo taken November 30, 2011 by Sergio Salinas.

Inside front-cover:
Top: Aerial photo of Alberca de los Espinos maar crater from the south. Photo taken February 7, 2010 by Claus Siebe.
Bottom: Aerial photo of Malpaís Prieto, the youngest lava flow in the Zacapu basin area. Photo taken from the southeast, February 7, 2010 by Claus Siebe.

Page 35:
Top: Aerial photo of the Tendeparacua lava flow and town of Huaniqueo from the southwest. Photo taken November 30, 2011 by Sergio Salinas.
Bottom: Aerial photo of the Malpaís Prieto and Capaxtiro lava flows (W margin of Zacapu basin) from the east. Photo taken February 7, 2010 by Claus Siebe.

Page 36:
Top: Aerial photo of Juanyan scoria cone and town of Cherán from the west. Photo taken November 30, 2011 by Sergio Salinas
Bottom: Aerial photo of the Costo tuff ring (near Uruapan) from the southwest. Photo taken February 1, 2009 by Claus Siebe.

Inside back-cover:
Top: Aerial photo of Cerro Capaxtiro scoria cone from which the Zacapu lava flow field emanated. Photo taken from the north, February 7, 2010 by Claus Siebe.
Bottom: Aerial photo of volcanic scoria quarry near Capula. The flat green area in the center is the remnant of the former crater floor of a young scoria cone. Photo taken from the East, November 30, 2011 by Claus Siebe.

Back-cover:
Top: Aerial photo of Paricutin crater from the southwest. Photo taken February 1, 2009 by Claus Siebe.
Bottom: Painting of Paricutin by Dr. Atl.

Tendeparacua lava flows

Capaxtiro and Malpaís Prieto

Juanyan and Cherán

Costo tuff ring

We acknowledge our sponsors for their support to this meeting:

UNIVERSIDAD NACIONAL
AUTÓNOMA DE MÉXICO

http://maar2014.geociencias.unam.mx